Ewolucja i pulsacje

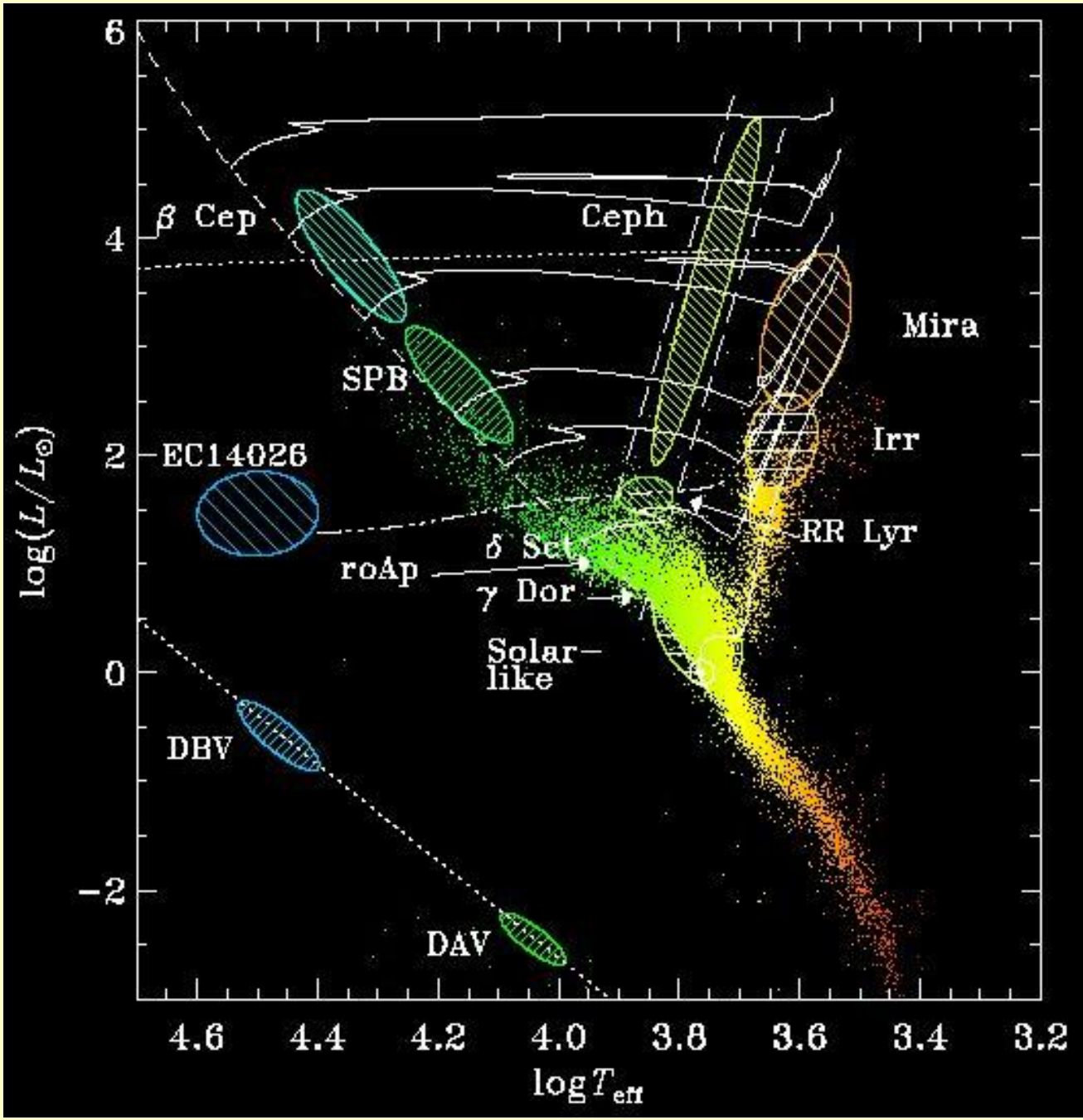

J. Christensen-Dalsgaard

Równania budowy wewnętrznej gwiazd

Table 24.1 Basic equations in Eulerian and Lagrangian forms

	$\frac{dP}{dr}$	$=$	$-\frac{GM_r}{r^2}\varrho$	$\frac{dP}{dM_r}$	$=$	$-\frac{GM_r}{4\pi r^4}$
	$\frac{dM_r}{dr}$	$=$	$4\pi r^2\varrho$	$\frac{dr}{dM_r}$	$=$	$\frac{1}{4\pi\varrho r^2}$
	$\frac{dL_r}{dr}$	$=$	$4\pi r^2\varrho(\varepsilon+\varepsilon_{\text{grav}}-\varepsilon_\nu)$	$\frac{dL_r}{dM_r}$	$=$	$(\varepsilon+\varepsilon_{\text{grav}}-\varepsilon_\nu)$
rad :	$\frac{dT}{dr}$	$=$	$-\frac{3\kappa\varrho}{4acT^3}\frac{L_r}{4\pi r^2}$	$\frac{dT}{dM_r}$	$=$	$-\frac{GM_rT}{4\pi r^4P}\nabla_{\text{rad}}$
conv :	$\frac{dT}{dr}$	$=$	$\frac{\Gamma_2-1}{\Gamma_2}\frac{T}{P}\frac{dP}{dr}$	$\frac{dT}{dM_r}$	$=$	$-\frac{GM_rT}{4\pi r^4P}\nabla_{\text{ad}}$

Maeder 2008

Równania budowy wewnętrznej gwiazd

$$\frac{dP}{dM_r} = -\frac{GM_r}{4\pi r^4}$$

$$\frac{dr}{dM_r} = \frac{1}{4\pi\varrho\, r^2}$$

$$\frac{dL_r}{dM_r} = (\varepsilon + \varepsilon_{\text{grav}} - \varepsilon_\nu)$$

$$\frac{dT}{dM_r} = -\frac{GM_r T}{4\pi r^4 P}\nabla_{\text{rad}}$$

$$\frac{dT}{dM_r} = -\frac{GM_r T}{4\pi r^4 P}\nabla_{\text{ad}}$$

Maeder 2008

κ OPAL GN93 (Livermore, 1996):

Instability domains

in the Upper MS

X=0.70, Z=0.02

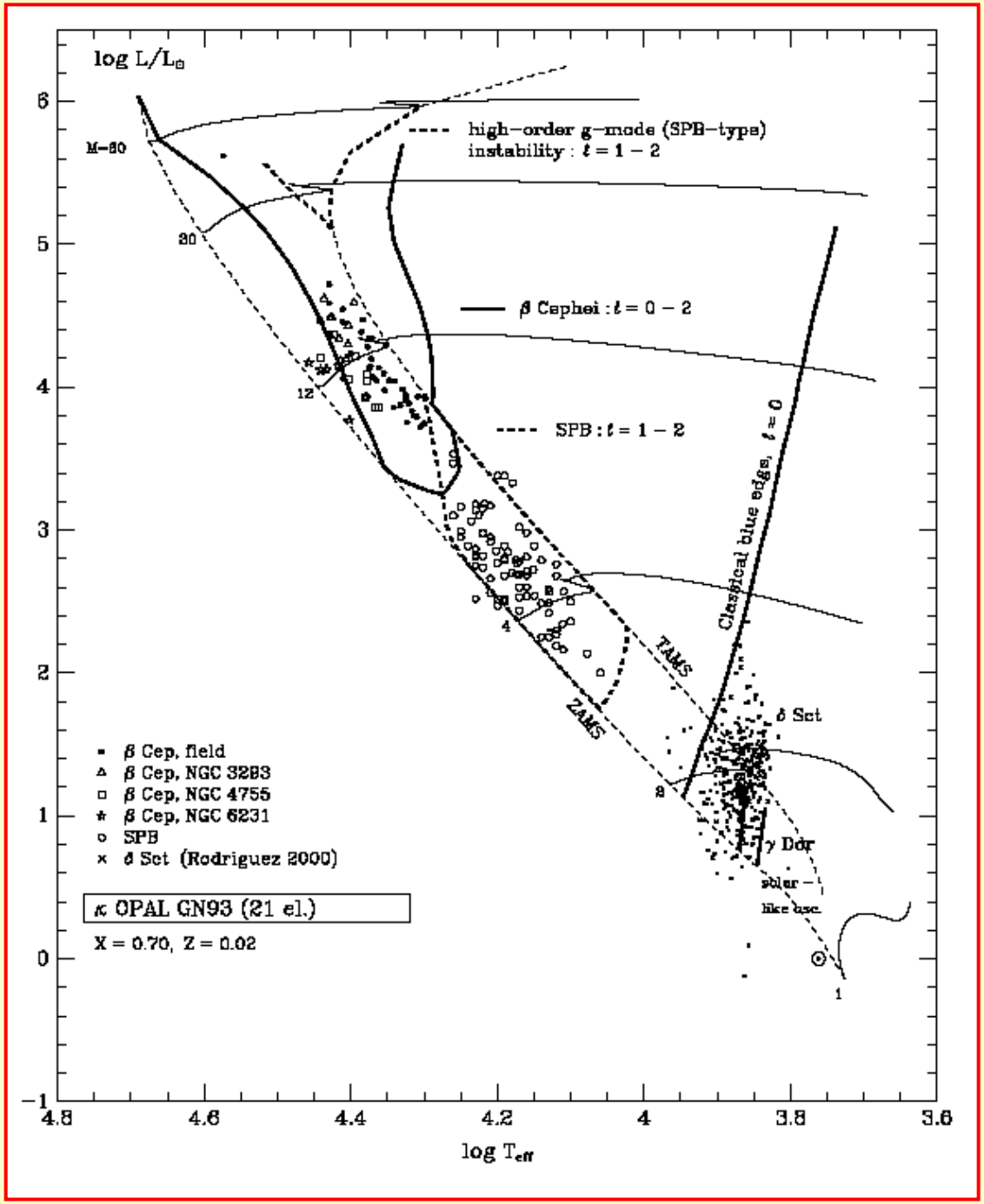

Pamyatnykh, 1999, Acta Astr., 49, 119

Effect of changes in the heavy element abundances on evolution and stability of the upper MS stars:

κ OPAL,
Z = 0.01, 0.015, 0.02

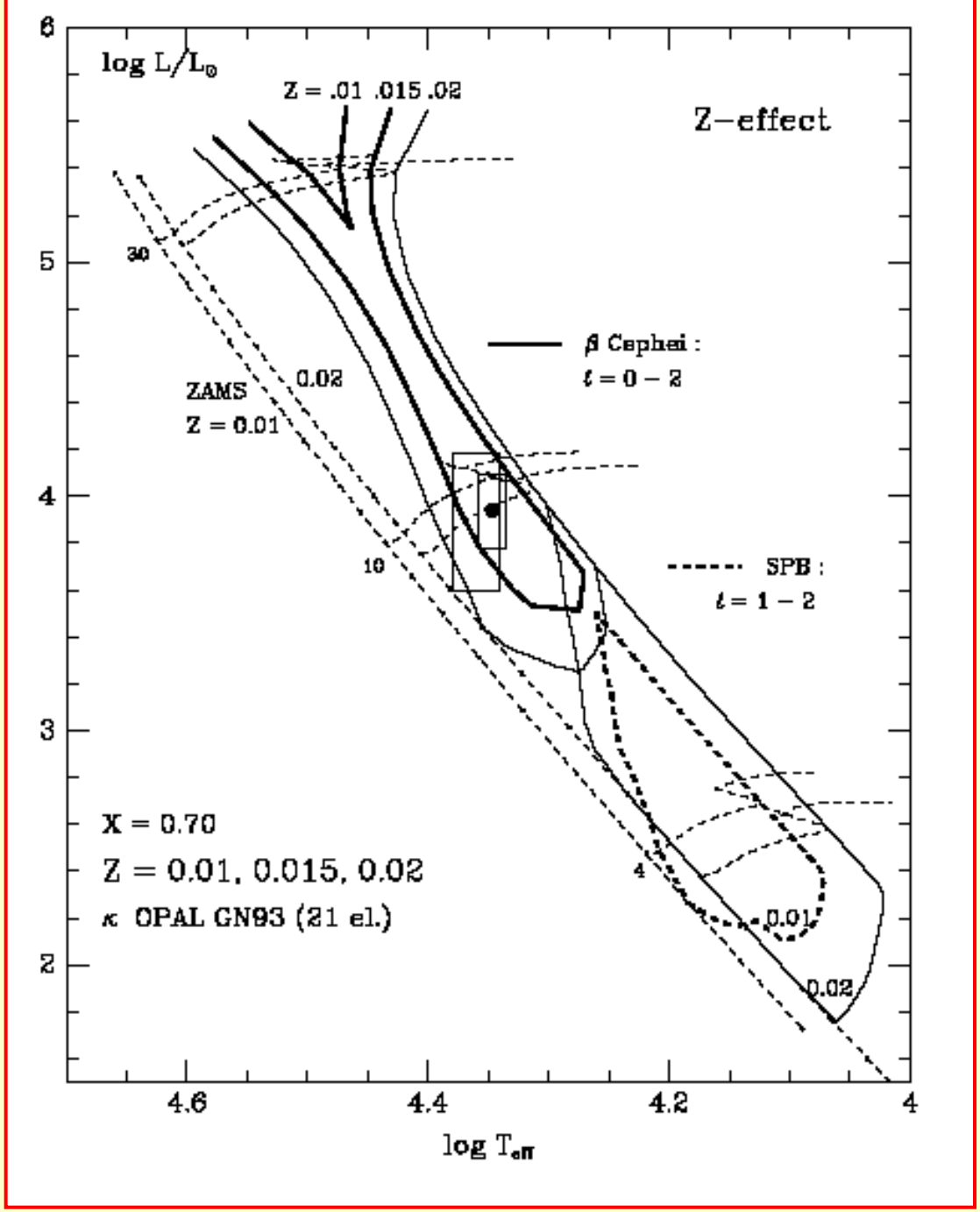

Pamyatnykh, 1999, Acta Astr., 49, 119

Opacity source	Z for β Cep instability
LAOL (< 1991)	no excitation
OPAL 1991	Z = 0.03-0.04
OPAL 1992	Z = 0.02-0.03
OPAL 1996	Z = 0.02-0.03
OP S92 >1993	Z = 0.02
OP A04 2005	Z = 0.01-0.02

With newest opacities and abundances it is possible to explain β Cep pulsations using models with significantly lower Z value than before.

Opacity behaviour at astrophysical conditions [κ OPAL 1996]

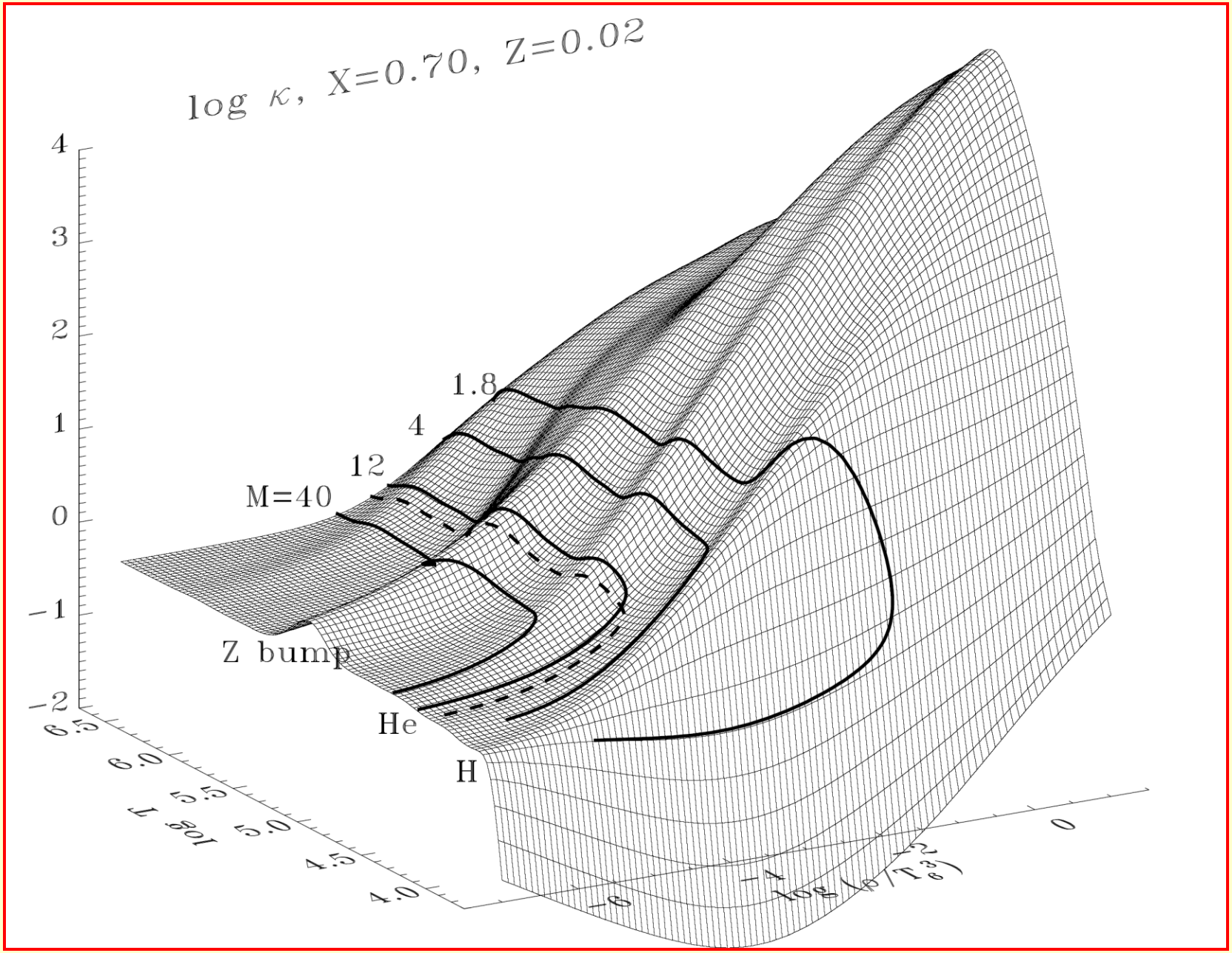

Pamyatnykh, 1999, Acta Astronomica, 49, 119

Wybrane modele gwiazd

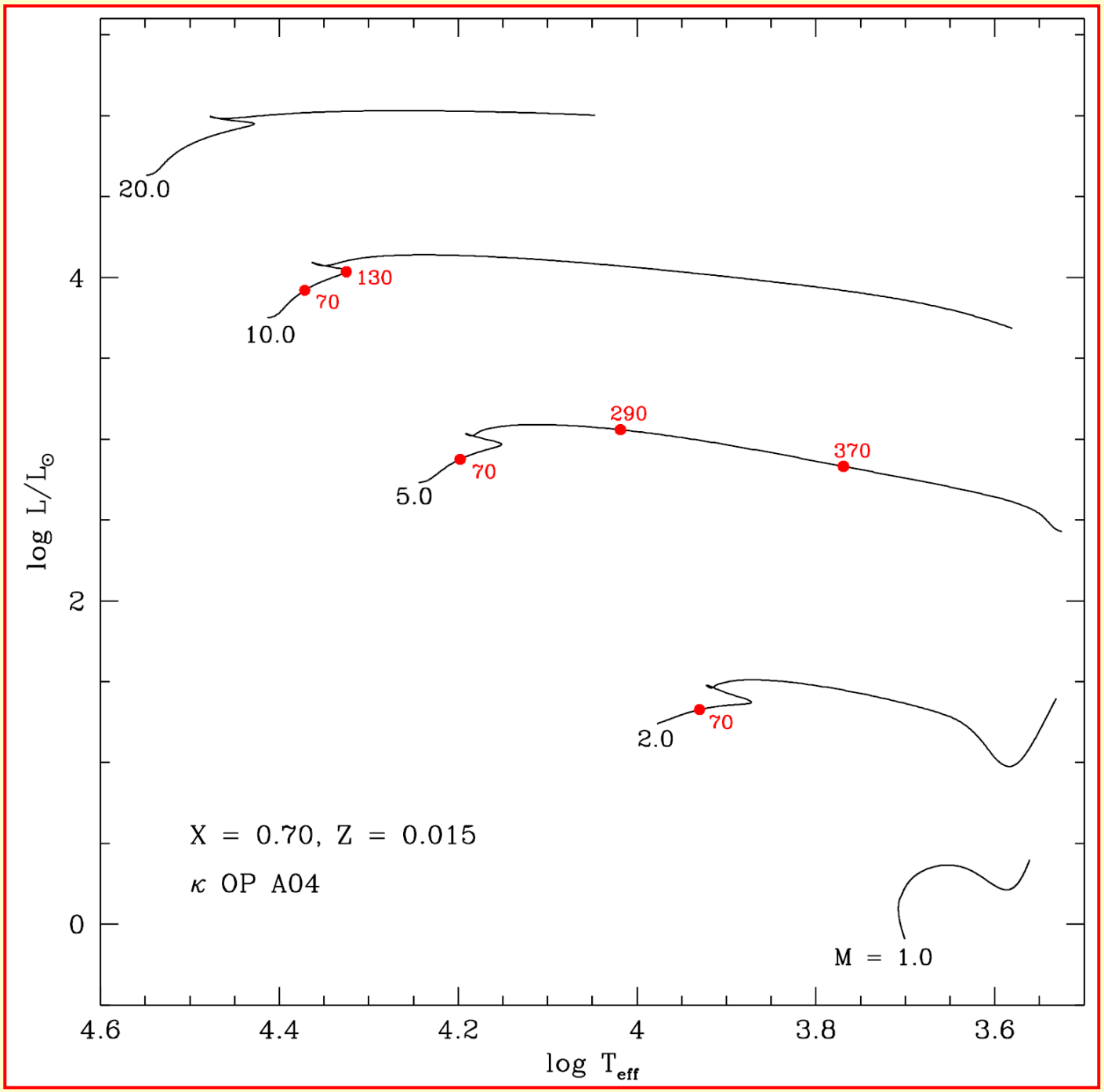

Regularities in theoretical frequency spectra:

- high-order p-modes:

$$\nu_{nl} \approx \Delta\nu \cdot \left(n + \frac{l}{2} + \alpha\right) - \frac{l(l+1)}{4\pi^2 n} \cdot f_c$$

$$\Delta\nu = \left(2\int \frac{dr}{c}\right)^{-1}, \quad f_c = \int \frac{dc}{dr} \cdot \frac{dr}{r}$$

large separation:

$$\nu_{nl} - \nu_{n-1,l} \approx \Delta\nu$$

small separation:

$$\nu_{nl} - \nu_{n-1,l+2} = \delta\nu_{nl} \approx -\frac{4l+6}{4\pi^2 n} \cdot f_c$$

- high-order g-modes:

$$\Pi_{nl} \approx \frac{n}{\sqrt{l(l+1)}} \cdot \Delta\Pi, \quad \Delta\Pi = 2\pi^2 \left(\int \frac{N}{r}\, dr\right)^{-1}$$

$$N = g\left(\frac{1}{\Gamma_1}\frac{d\ln P}{dr} - \frac{d\ln \rho}{dr}\right)$$

- Rotational splitting: (~ Goupil et al. 2000)

$$\nu_m = \nu_0 + m\left(1 - C_{nl}\right)\frac{\Omega}{2\pi} + \frac{\Omega^2}{2\pi\nu_0}\left(D_0 + m^2 D_1\right) + m\frac{\Omega^3}{\nu_0^2}T$$

$$\Rightarrow \frac{\nu_m - \nu_{m=0}}{m} = \frac{\Omega}{2\pi}\left(1 - C_{nl} + m\mu D_1 + \mu^2 T\right)$$

$$\mu = \frac{\Omega}{\nu_0}$$

- rotation rate:

$$\frac{\nu_m - \nu_{-m}}{2m} = \Omega\left(1 - C_{nl} + \mu^2 T\right)$$

Częstotliwości radialnych, dipolowych i kwadrupolowych oscylacji ewolucyjnych modeli gwiazd z M = 10 Msun (od ZAMS do TAMS)

Czerwone kropki - mody niestabilne

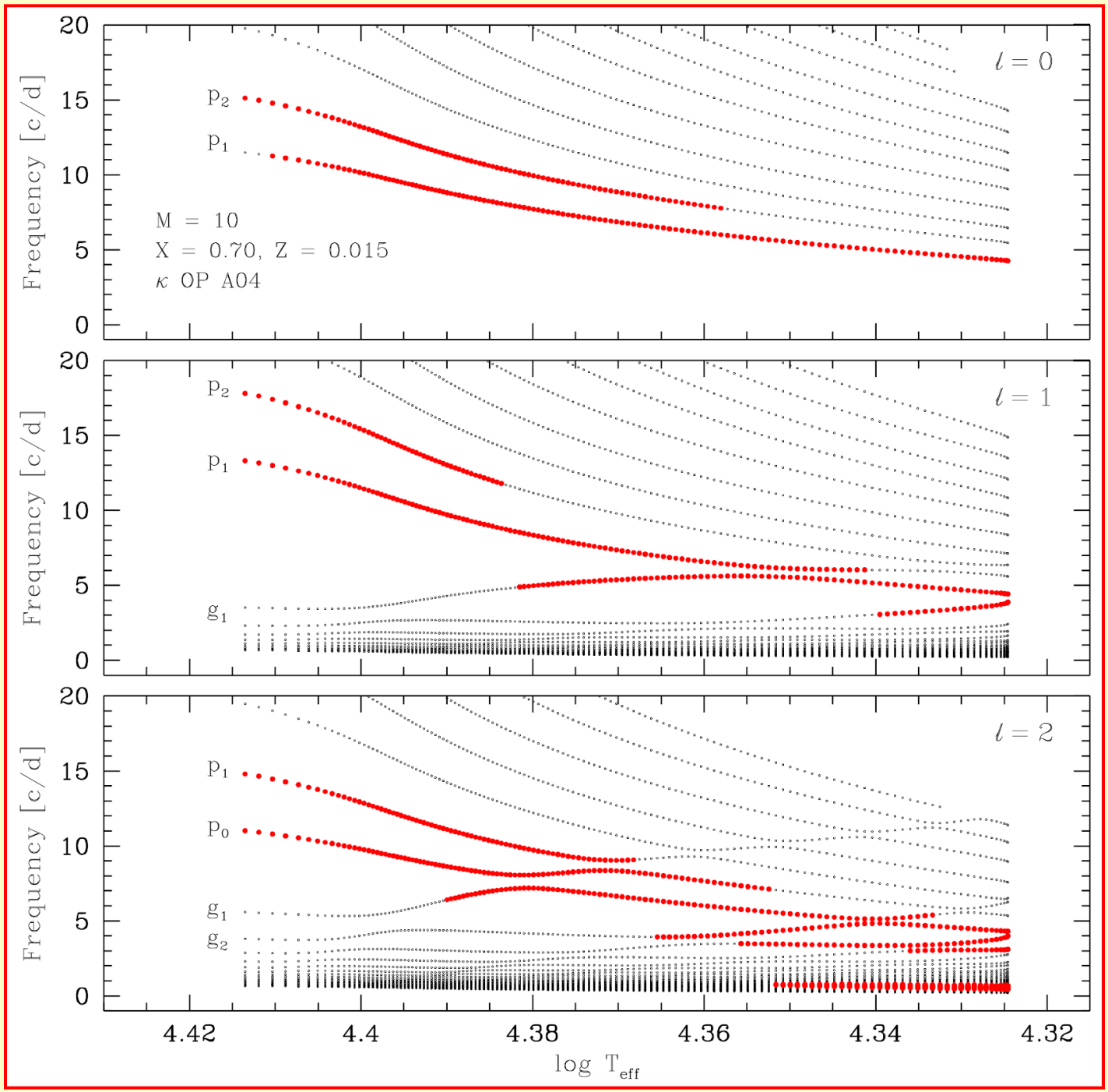

Jak poprzednio, ale w jednostkach bezwymiarowych:

$$\sigma = \omega / \sqrt{4\pi G \langle \rho \rangle}$$

ω – kołowa częstotliwość, $\omega = 2\pi\nu$

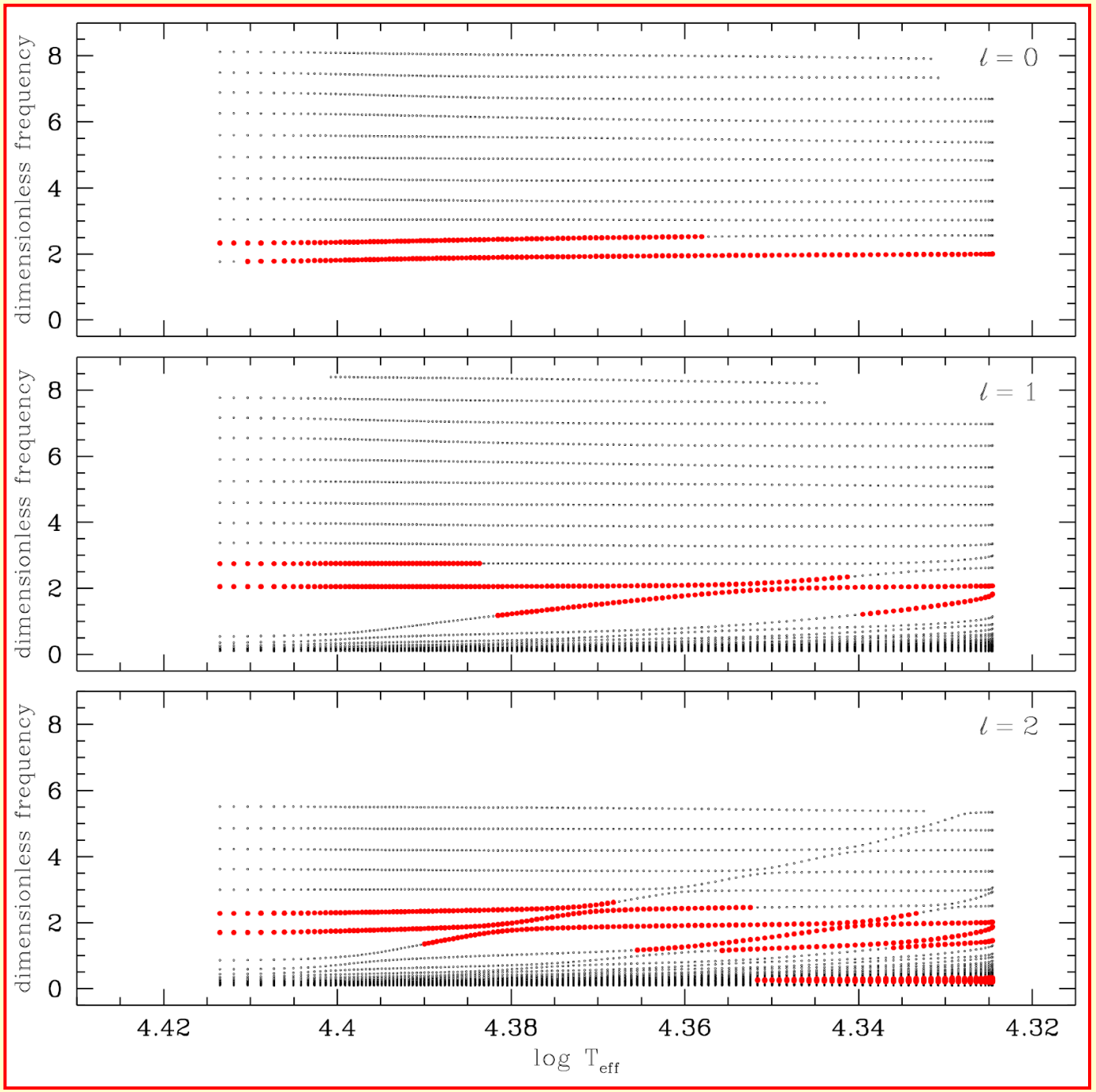

Okresy radialnych, dipolowych i kwadrupolowych oscylacji ewolucyjnych modeli gwiazd z M = 10 Msun (od ZAMS do TAMS)

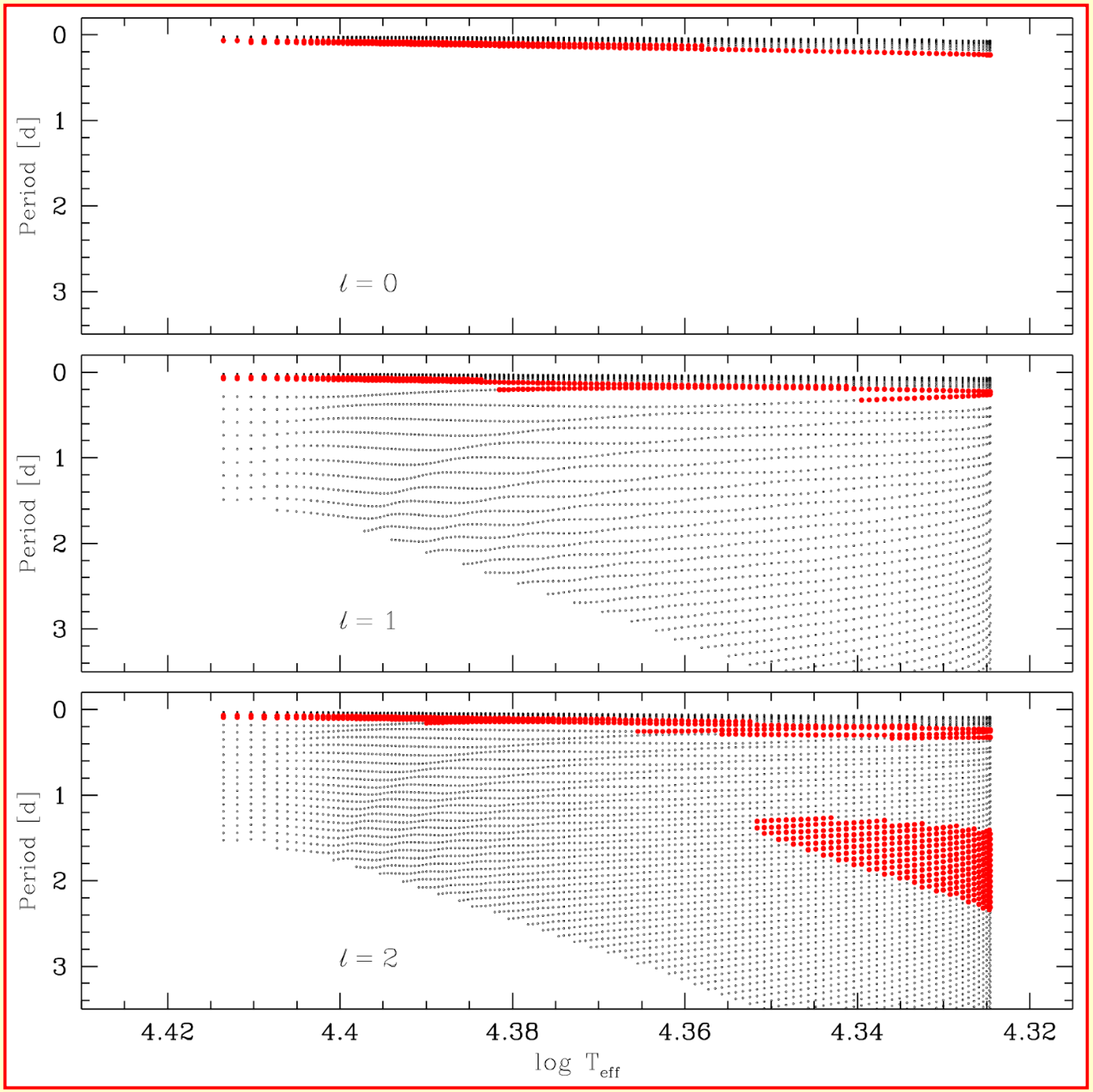

Lines of constant period in the HRD

Rough estimate of the position of the constant period lines in HR diagram:

$\Pi\sqrt{\rho} \sim const \Rightarrow \Pi \sim M^{-1/2} R^{3/2}$

$\Rightarrow M \sim R^3$ for const Π

$M \sim L^{1/3}$ (mass-luminosity relation for ~MS stars)

$\Rightarrow L \sim R^9$ for const Π

$L \sim R^2 T_e^4 \Rightarrow R \sim L^{1/2} T_e^{-2}$

$\Rightarrow L \sim L^{9/2} T_e^{-18}$ for const Π

$\Rightarrow L \sim T_e^5$

$\lg L \sim 5 \cdot \lg T_e$

Main sequence: $\frac{\Delta \lg L}{\Delta \lg T_e} \sim \frac{6.5}{0.9} \sim 7$

or $\lg L \sim 7 \cdot \lg T_e$

$\Rightarrow$ The constant period lines are, roughly, parallel to the main sequence. (they have slightly lower slope)

Wybrane modele gwiazd

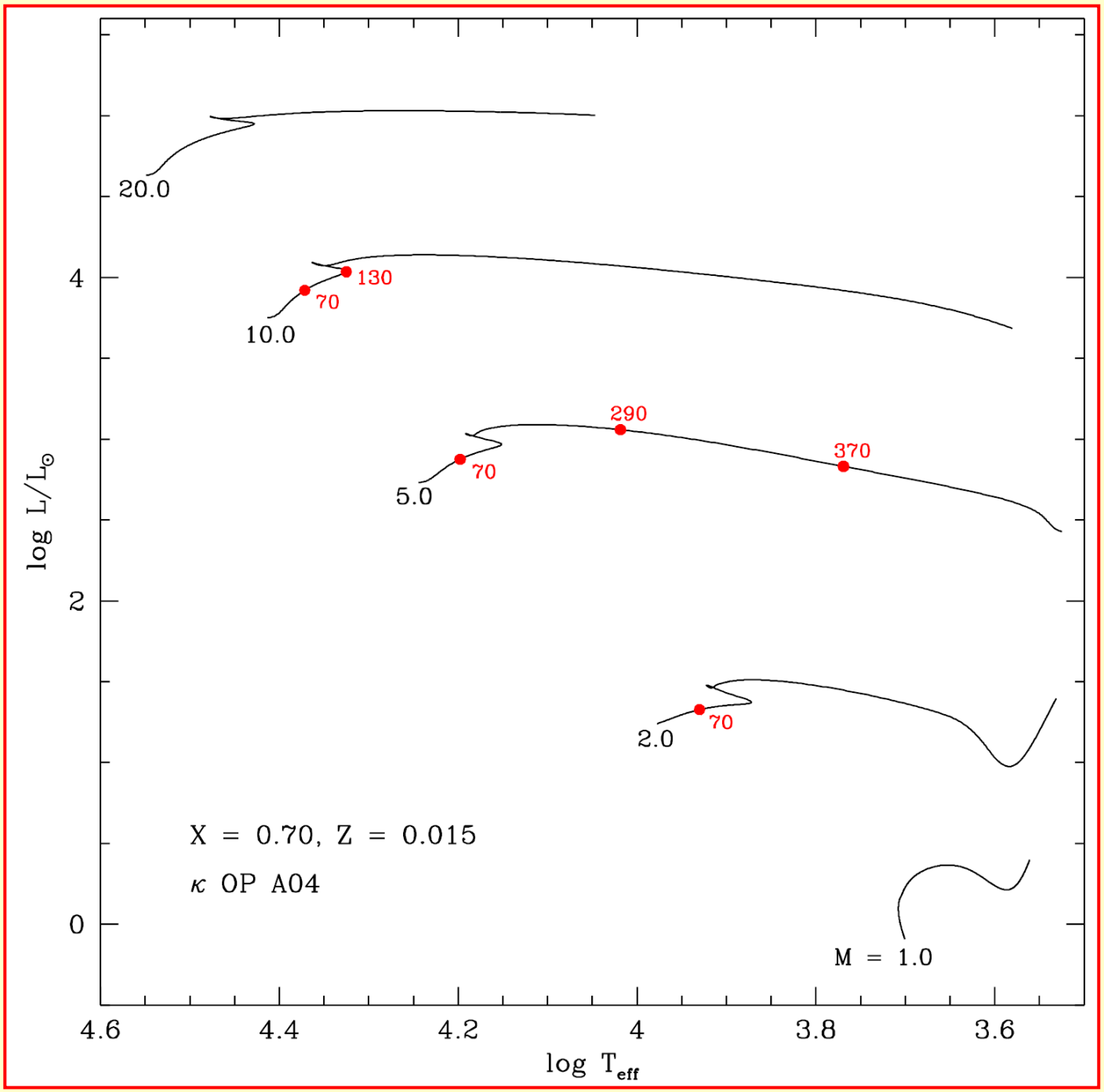

Differential work integral and density of kinetic energy for two modes in the 5 Msun model 370

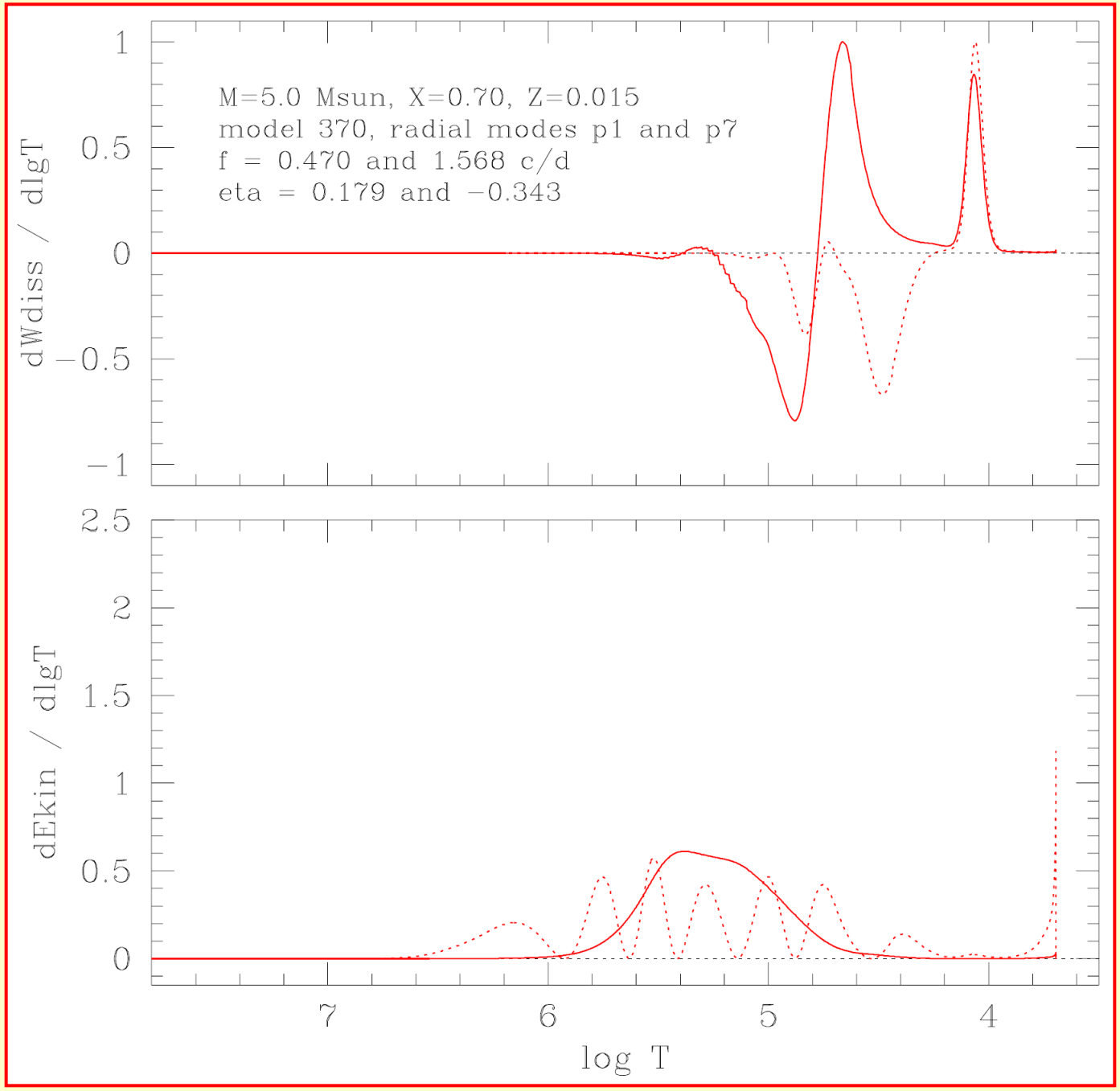

Differential work integral and pressure perturbation for two modes in the 5 Msun model 370

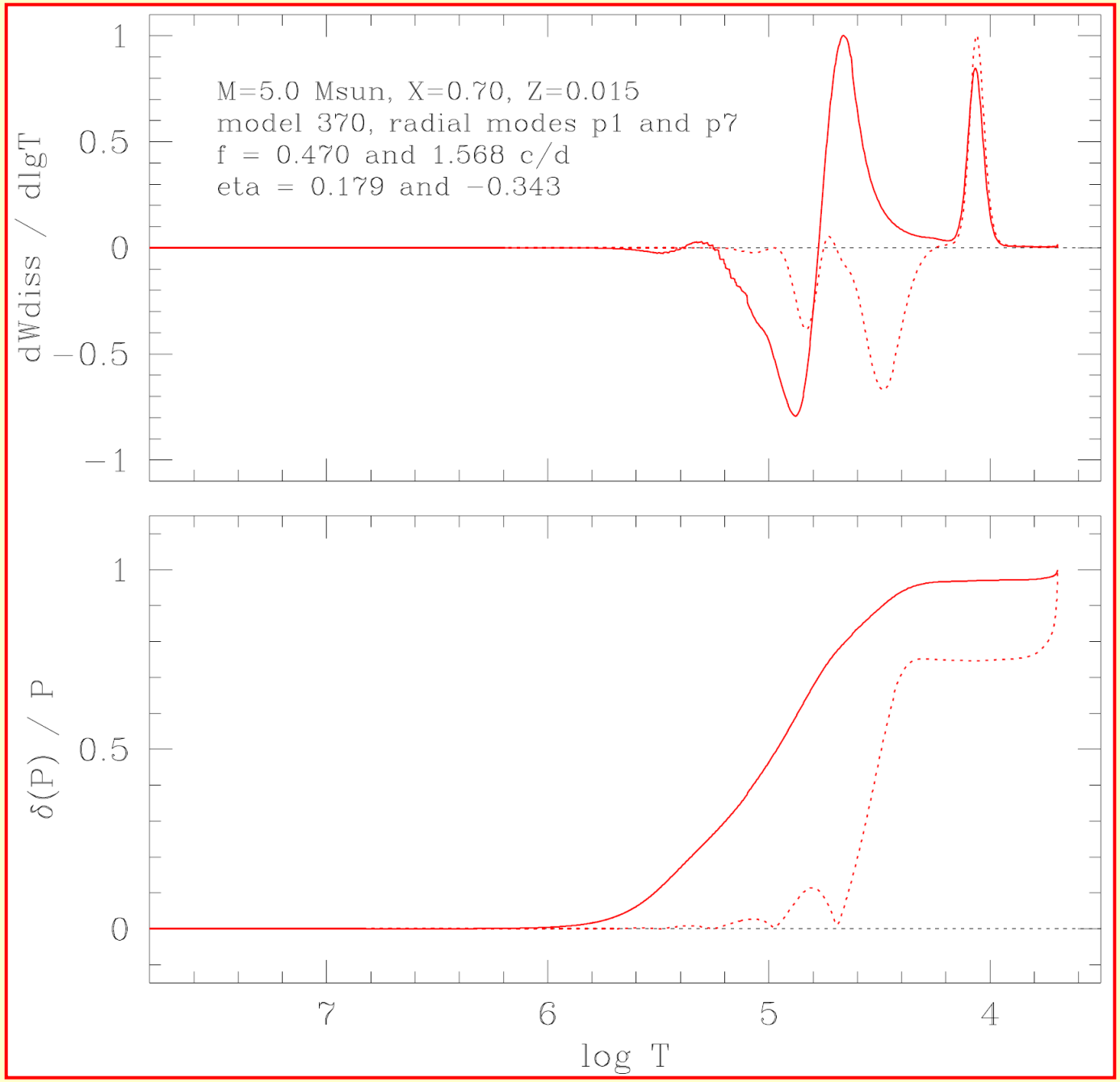

Wybrane modele gwiazd

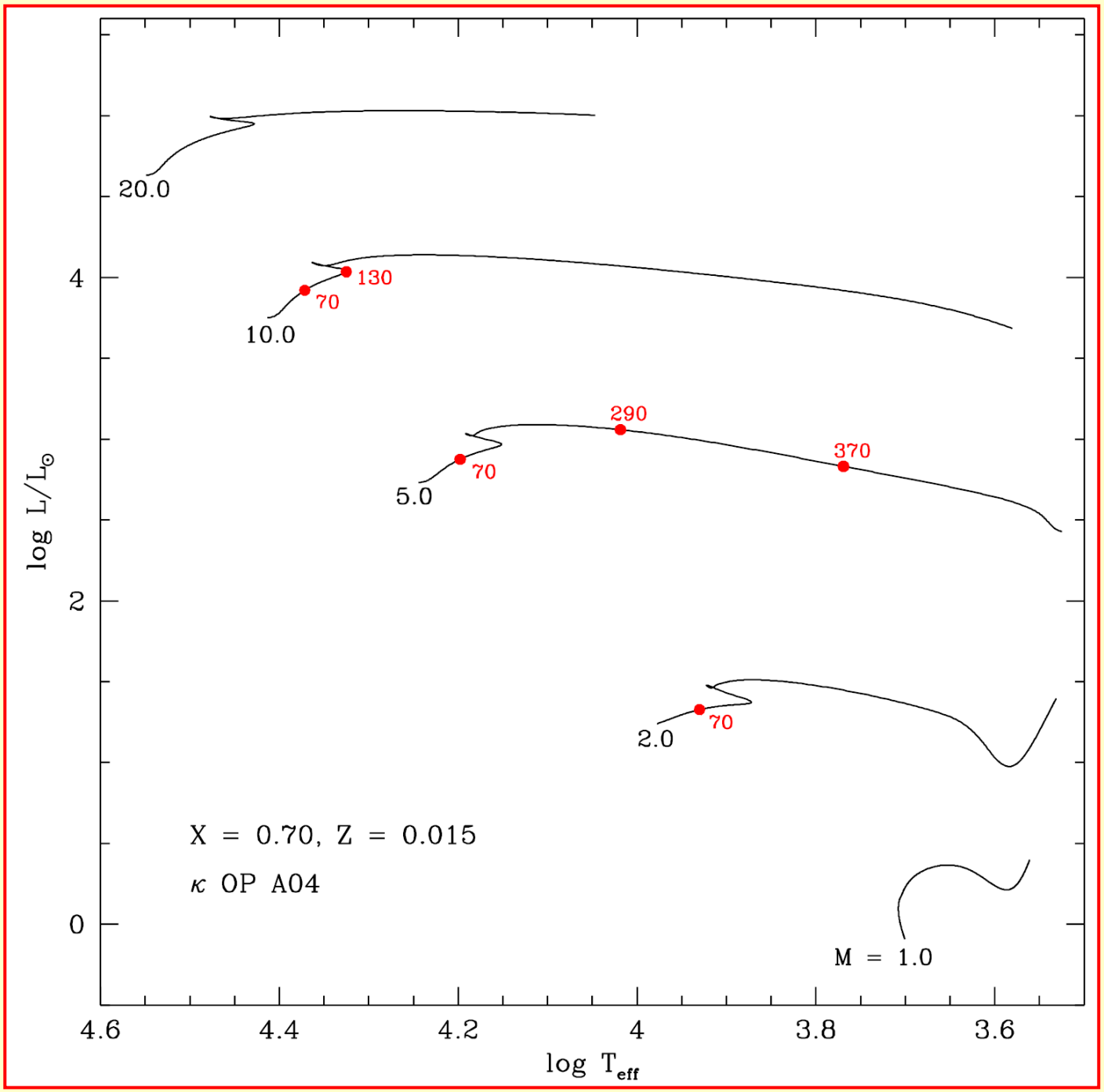

Differential work integral and density of kinetic energy for two modes in the 5 Msun model 290

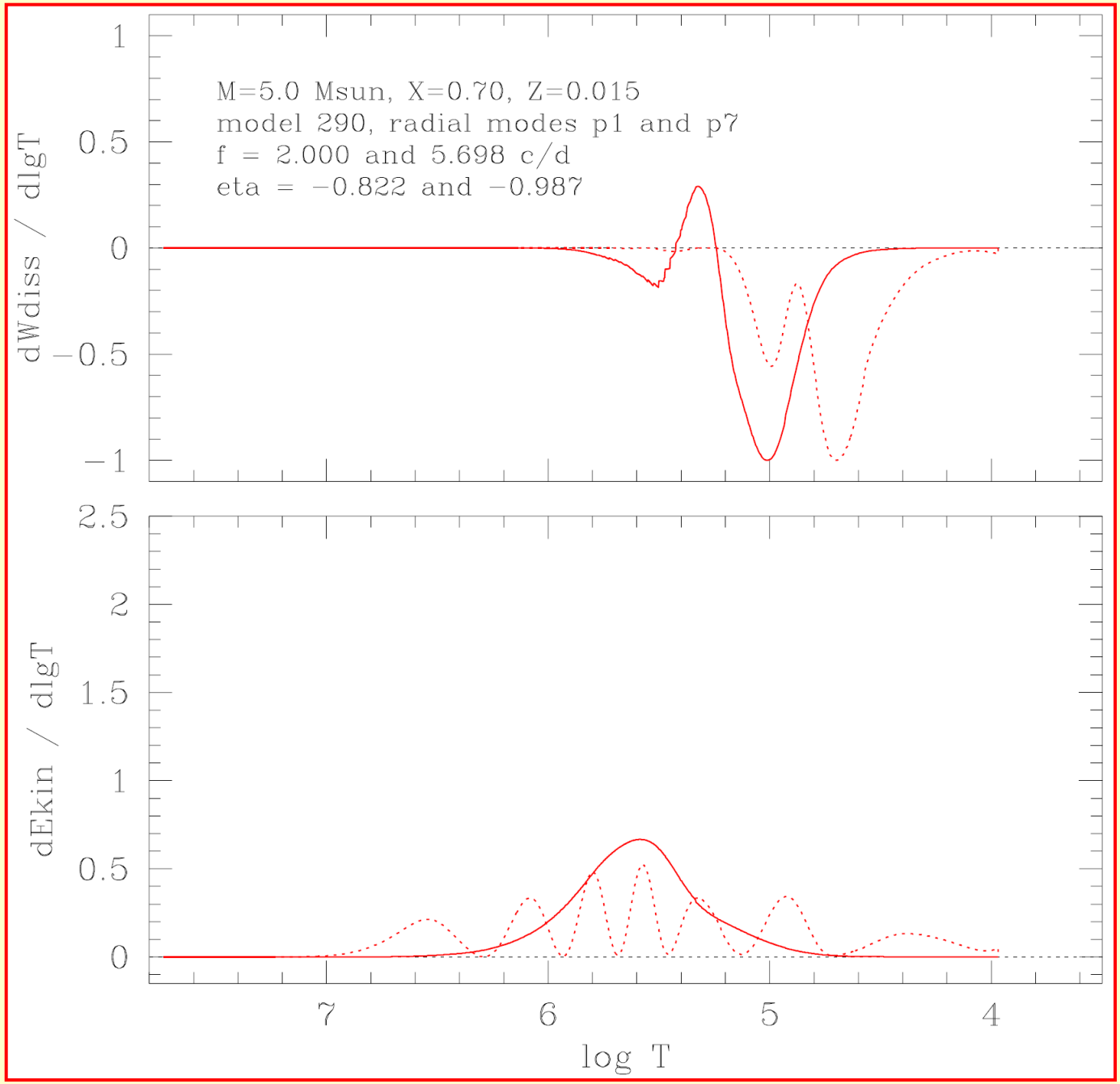

Differential work integral and pressure perturbation for two modes in the 5 Msun model 290

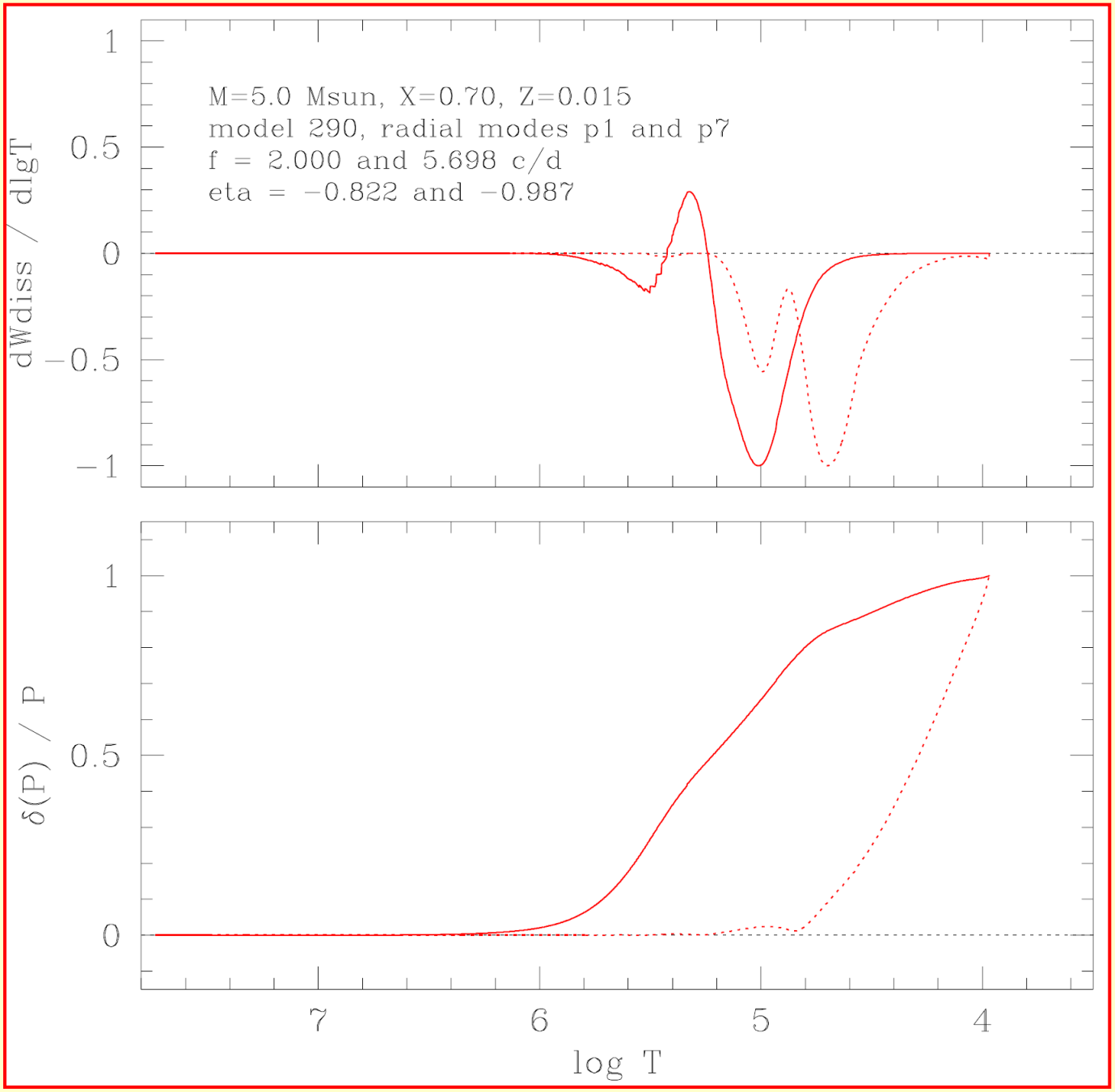

Wybrane modele gwiazd

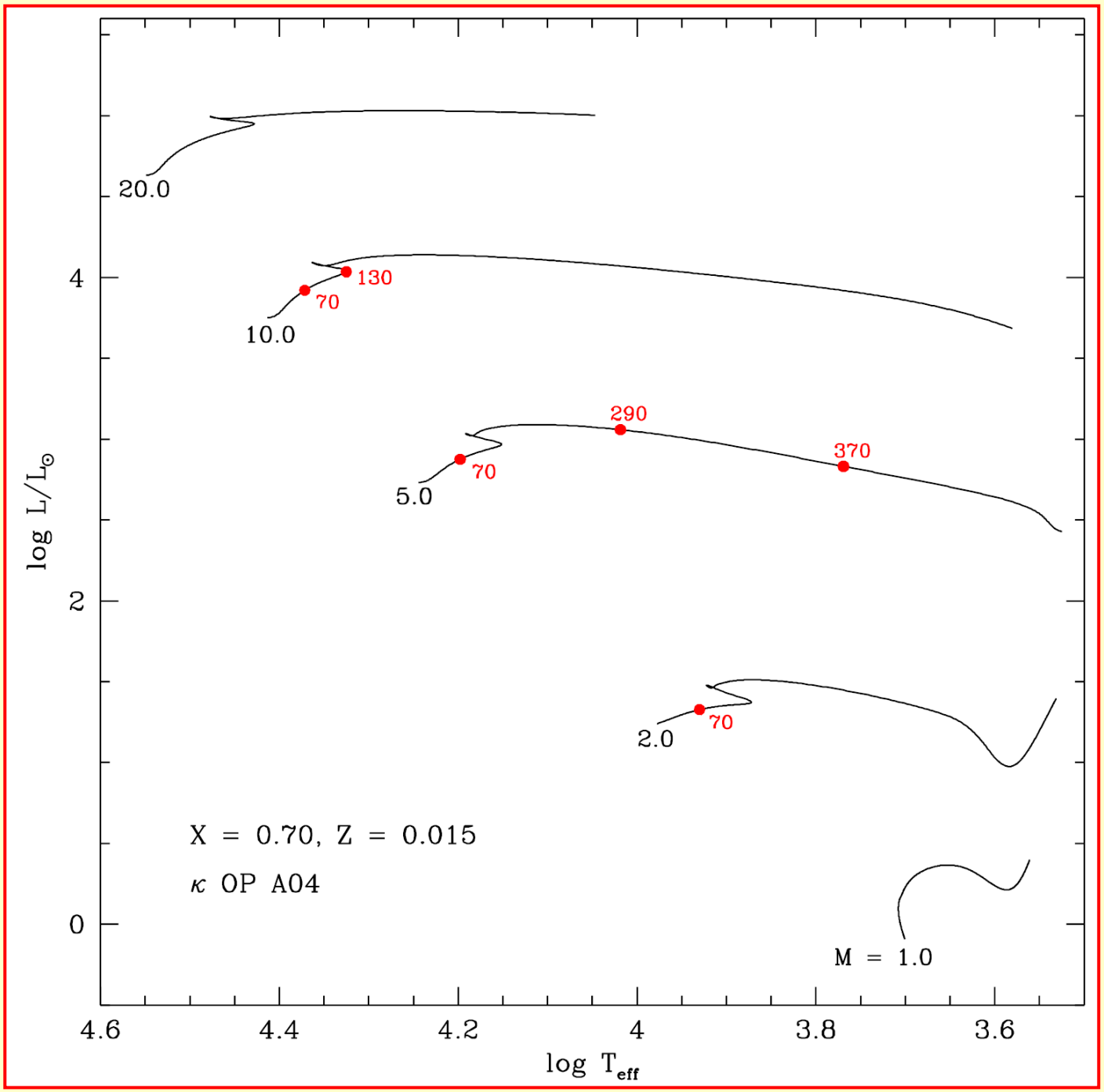

Differential work integral and density of kinetic energy for two modes in the 5 Msun model 70

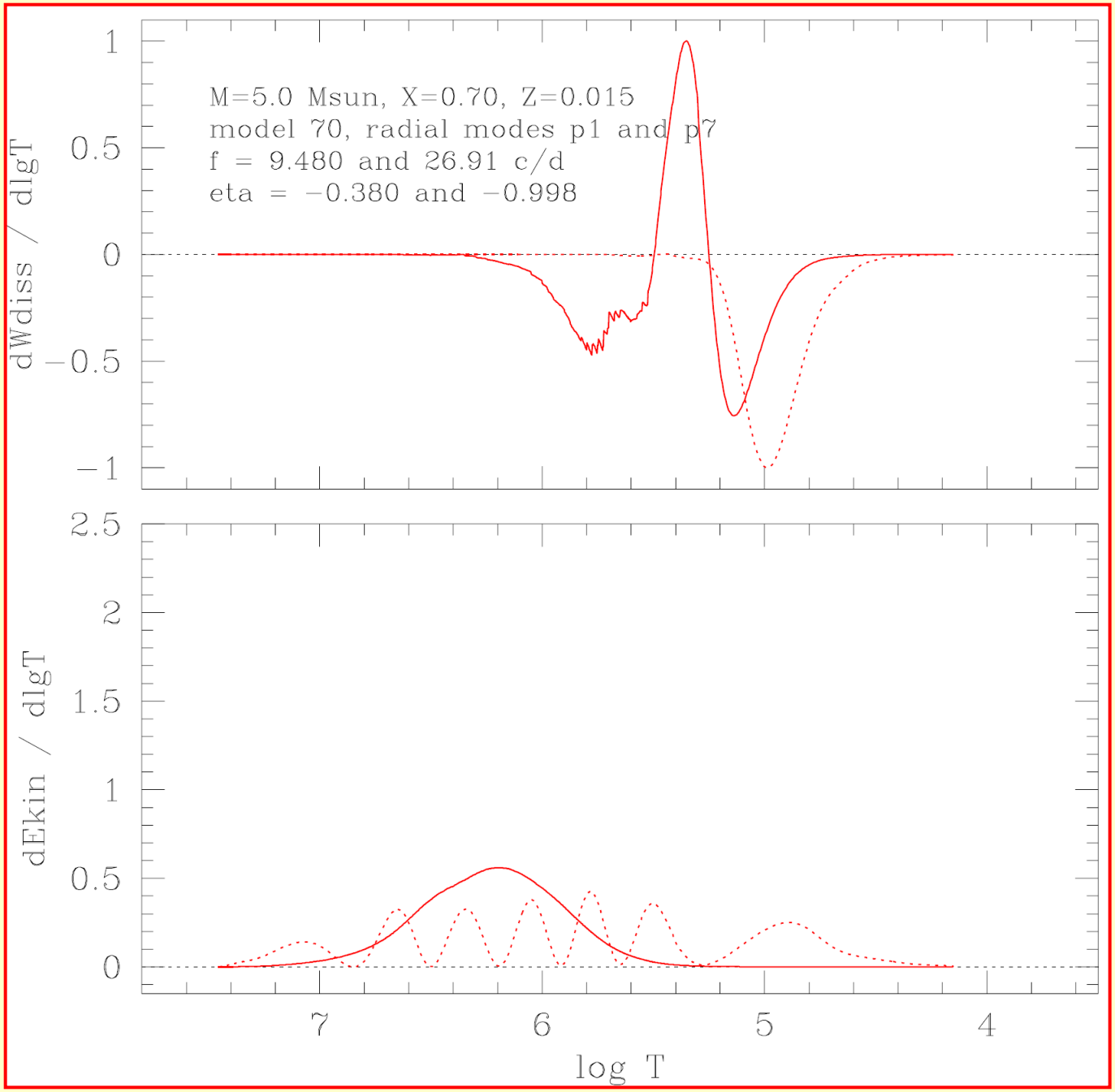

Differential work integral and pressure perturbation for two modes in the 5 Msun model 70

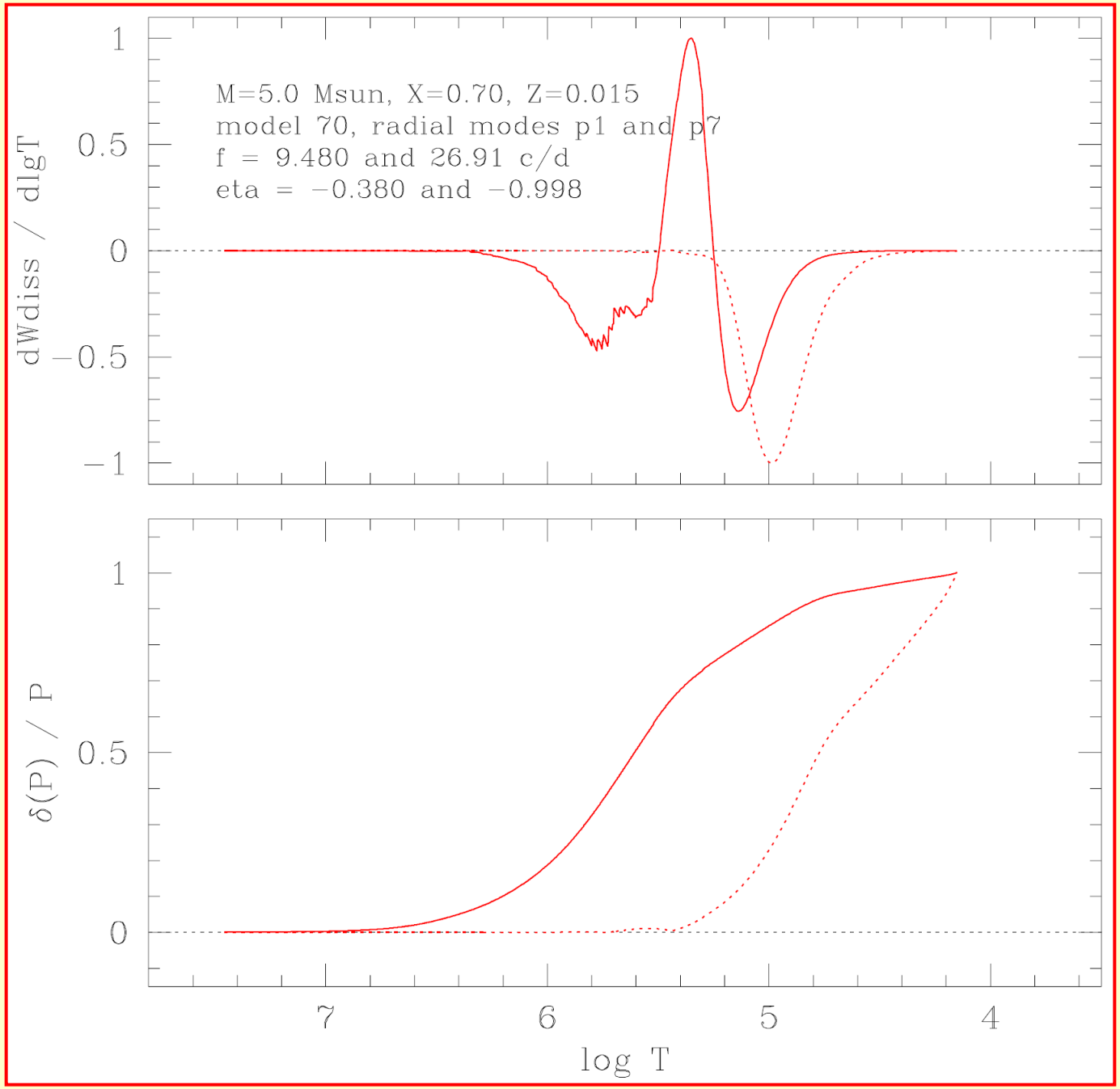

Wybrane modele gwiazd

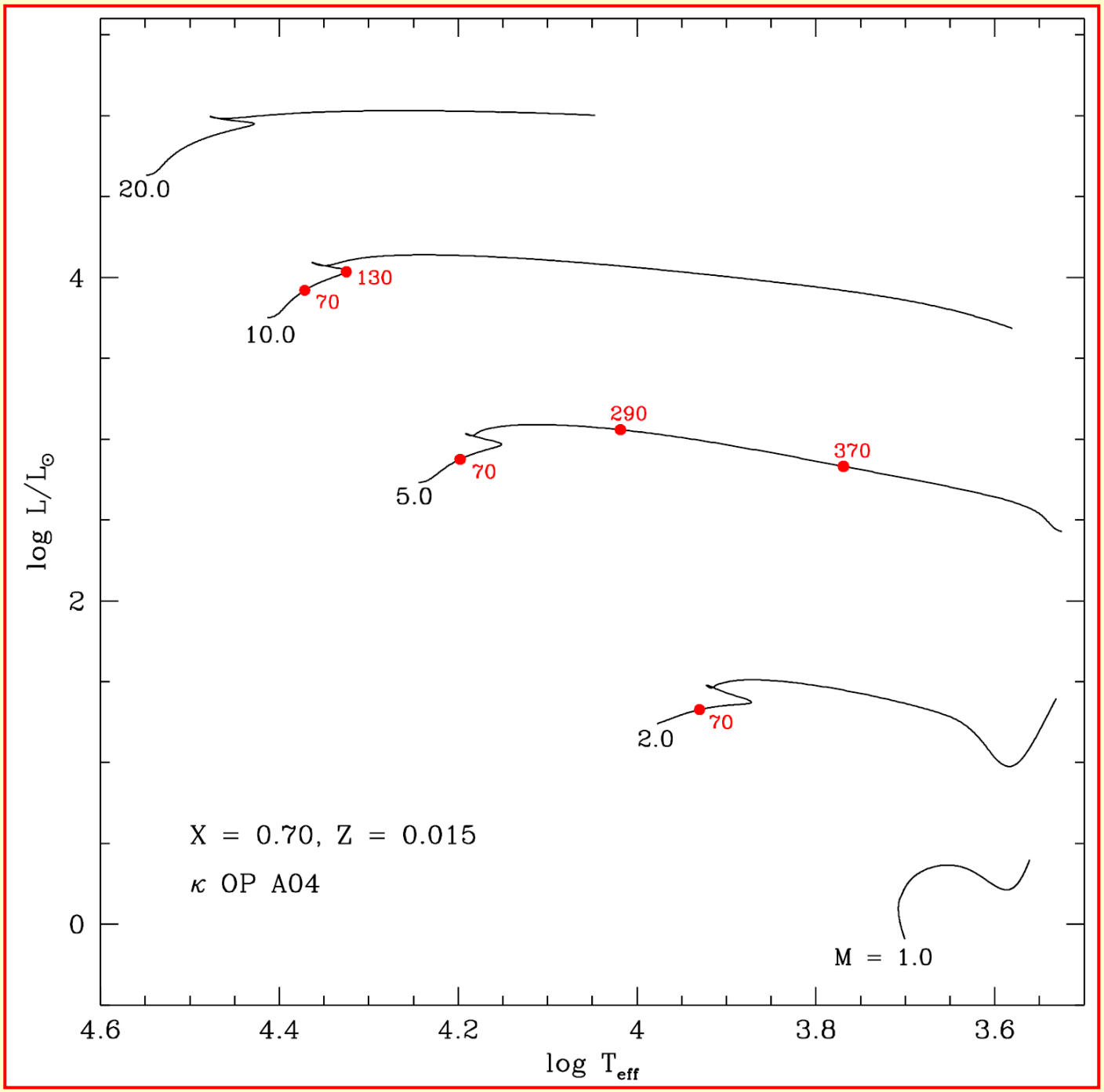

Differential work integral and density of kinetic energy for two modes in the 10 Msun model 70

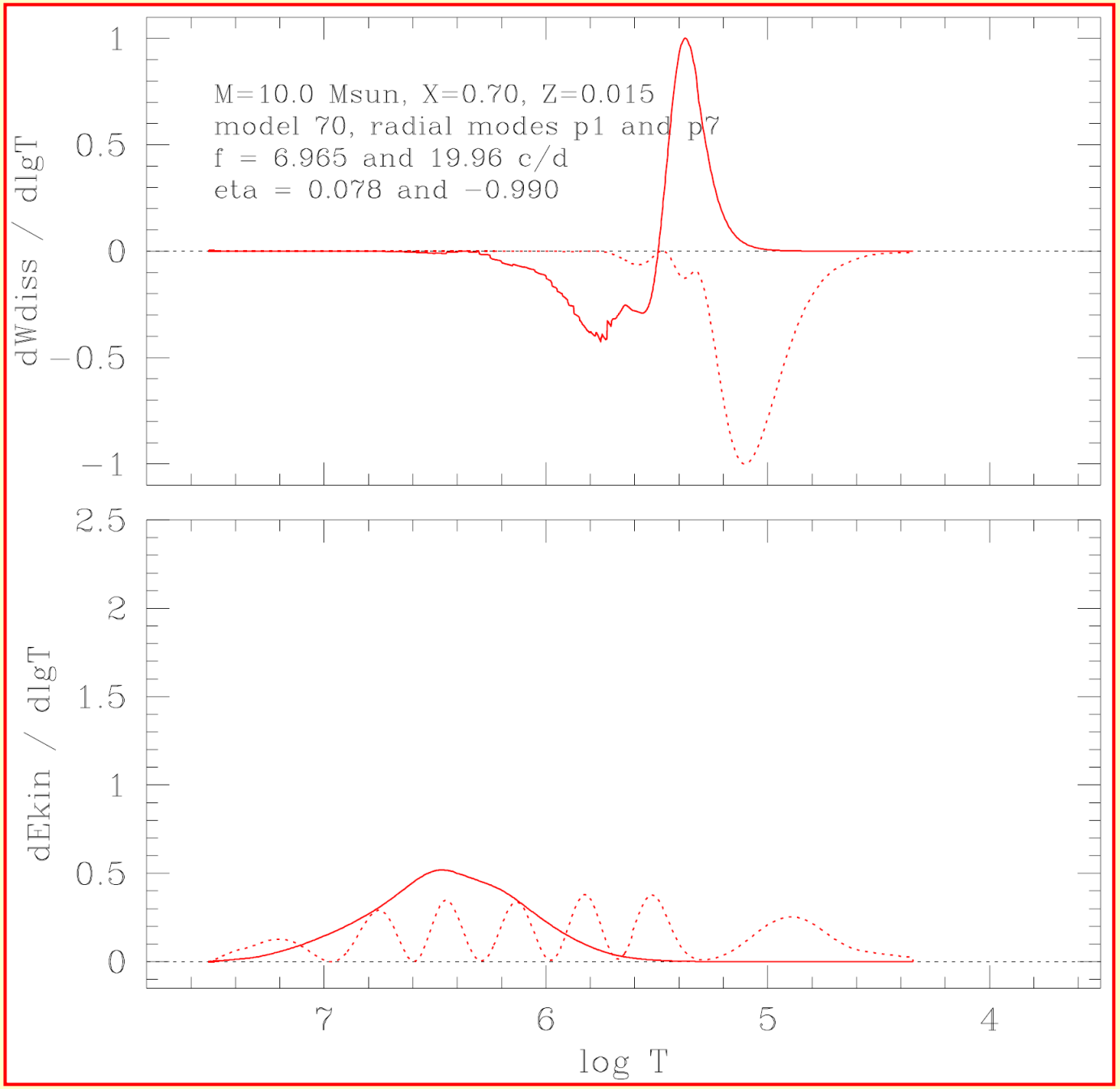

Differential work integral and pressure perturbation for two modes in the 10 Msun model 70

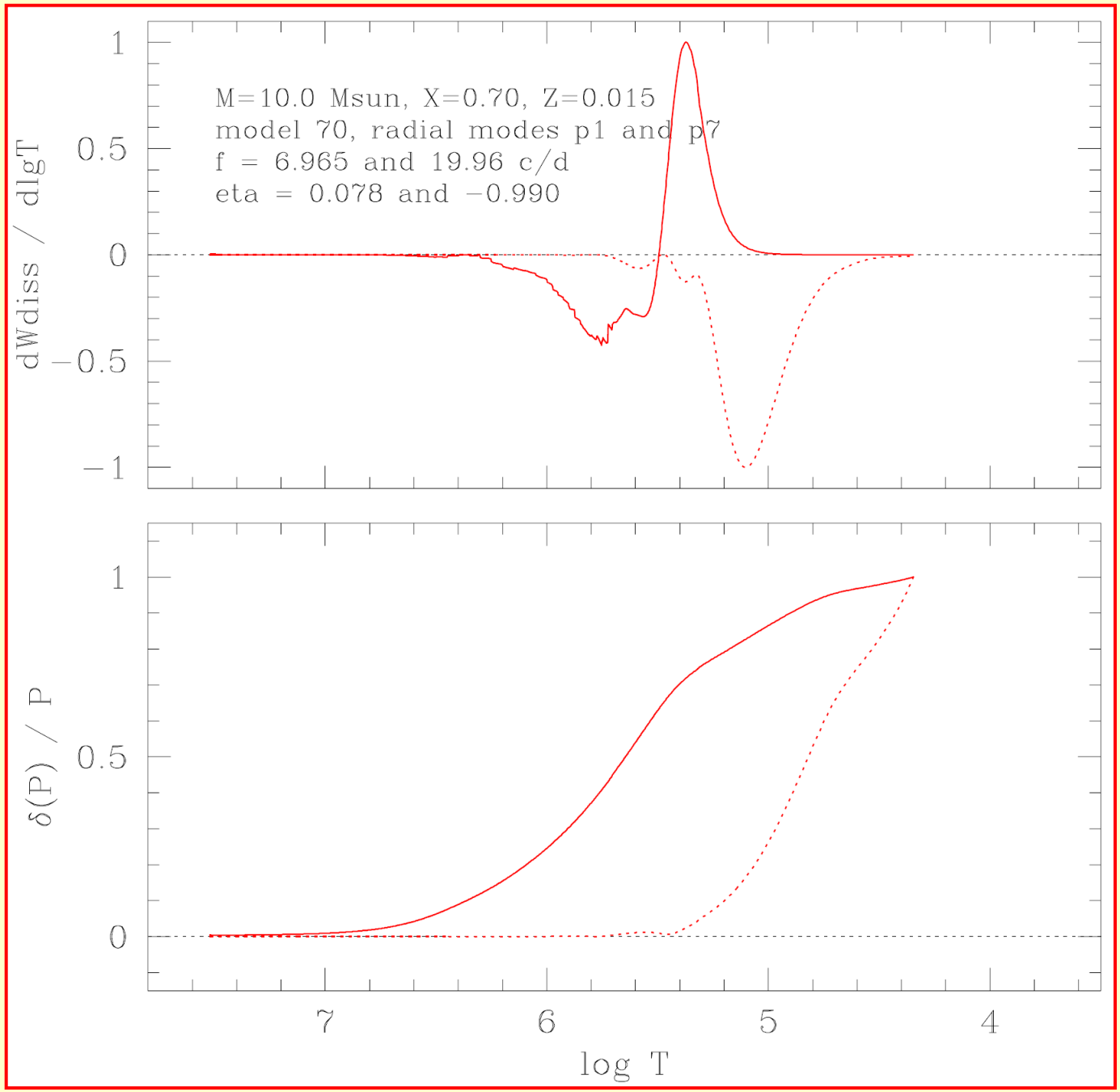

Wybrane modele gwiazd

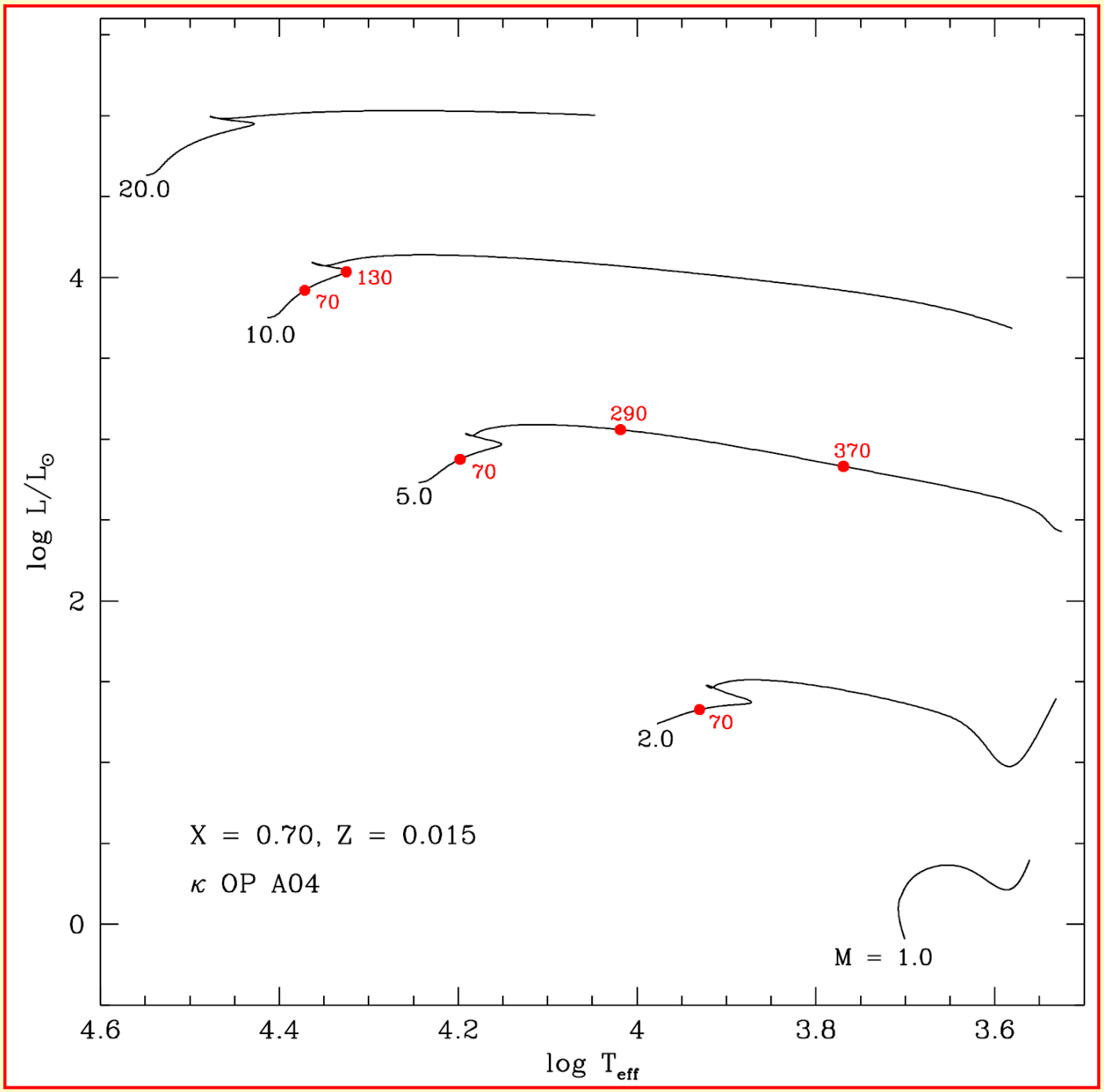

Differential work integral and density of kinetic energy for two modes in the 2 Msun model 70

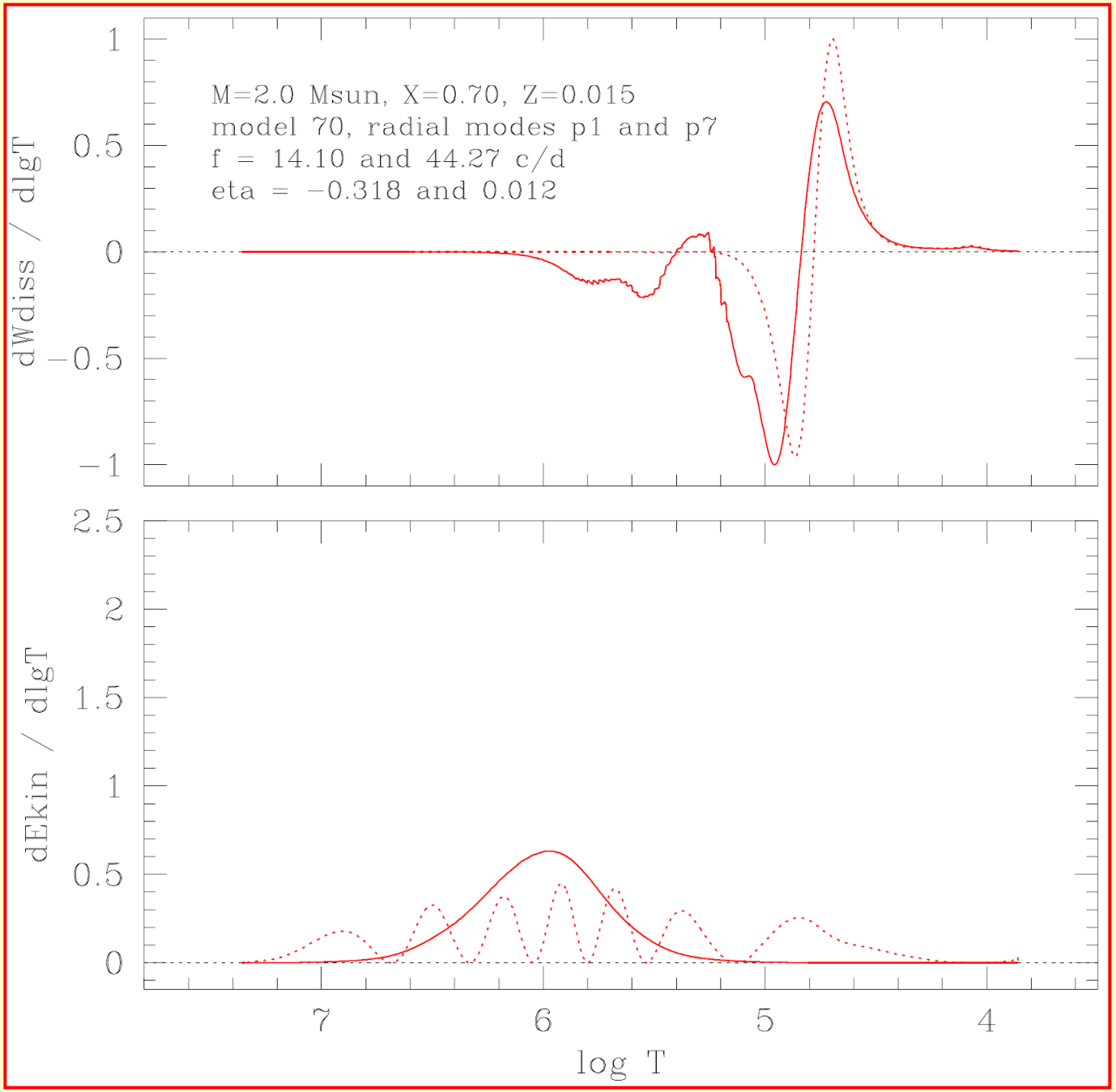

Differential work integral and pressure perturbation for two modes in the 2 Msun model 70

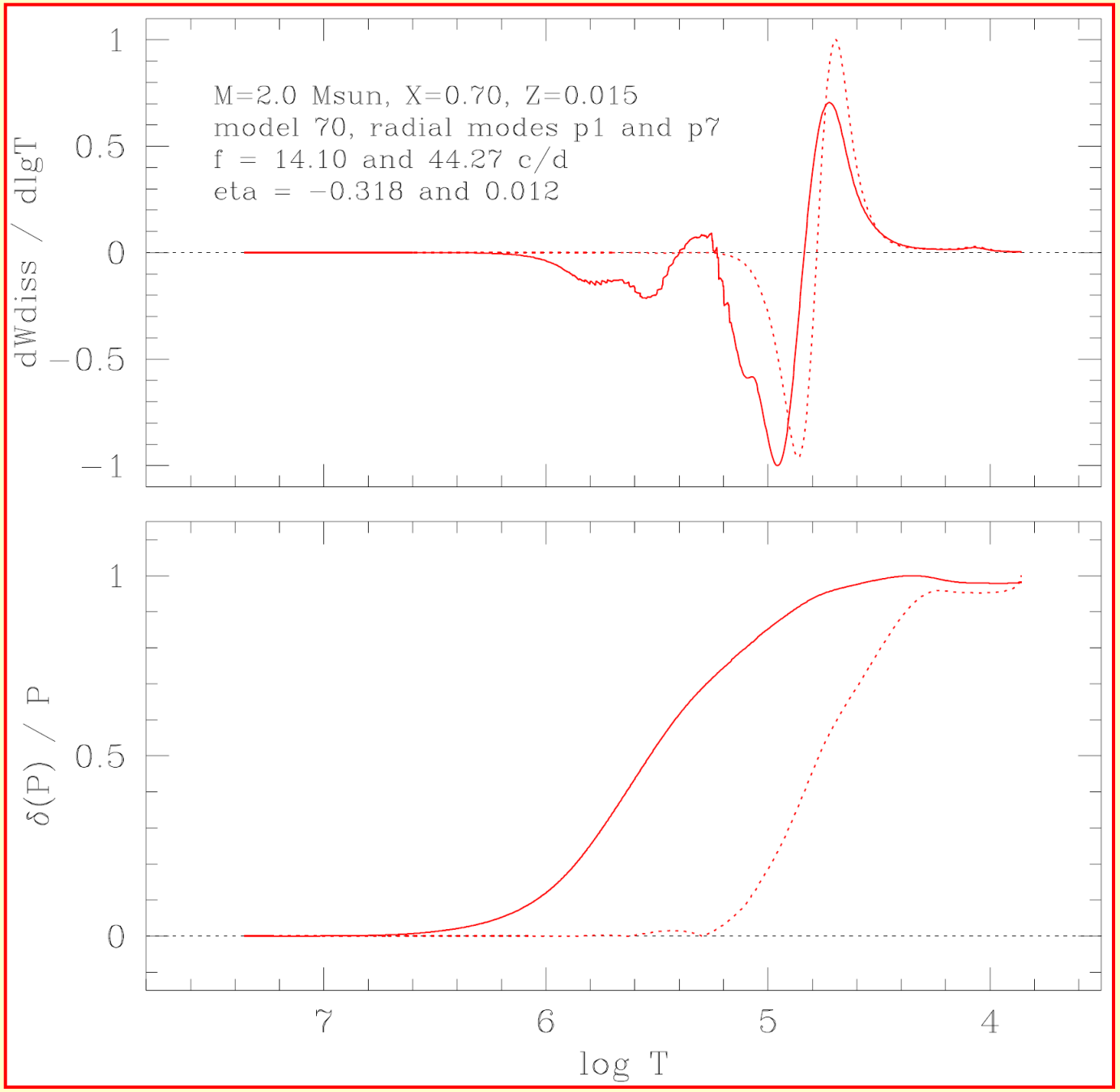

Wybrane modele gwiazd

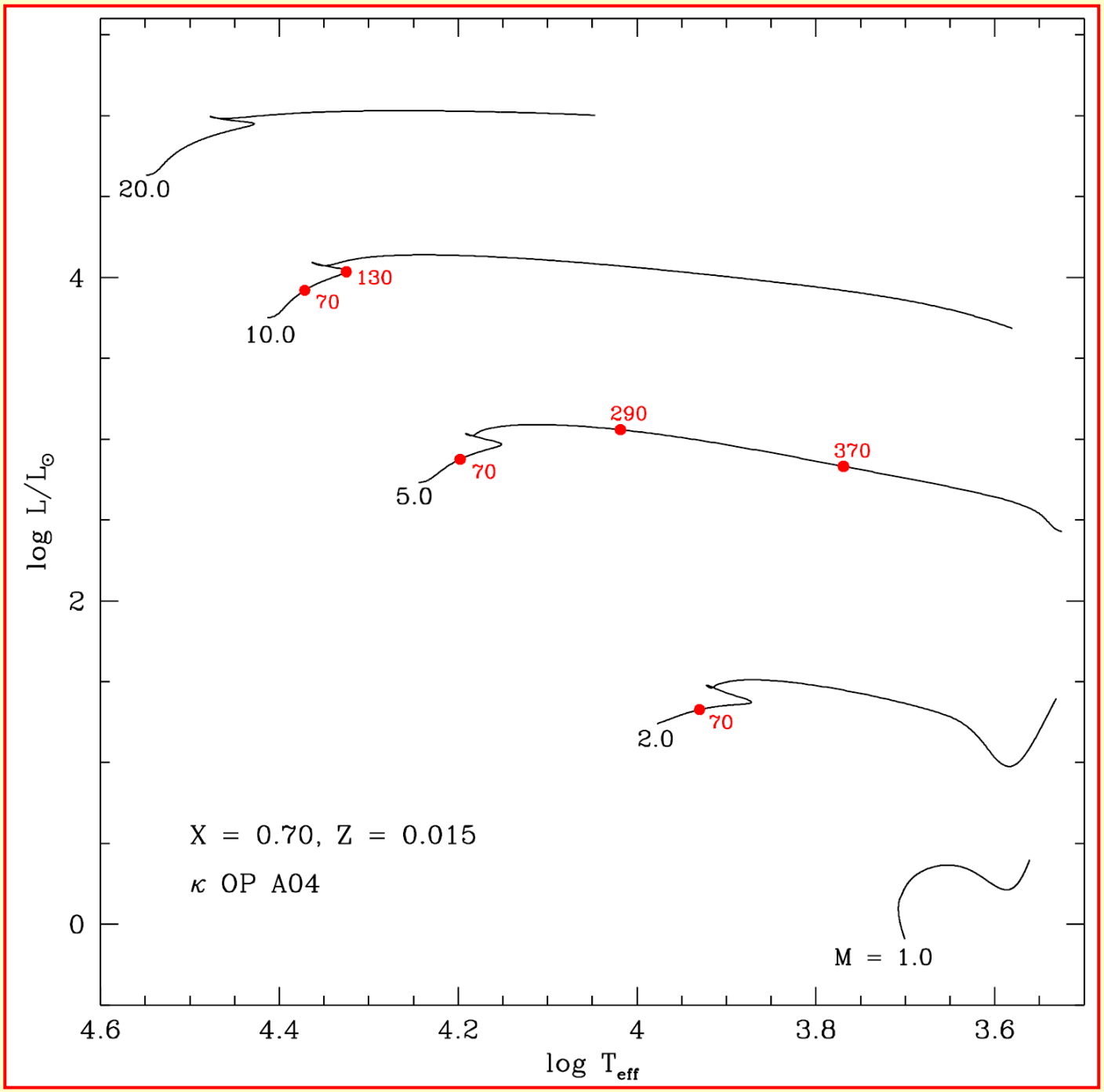

Perios of unstable high-order g-modes in the 5 Msun models on main sequence

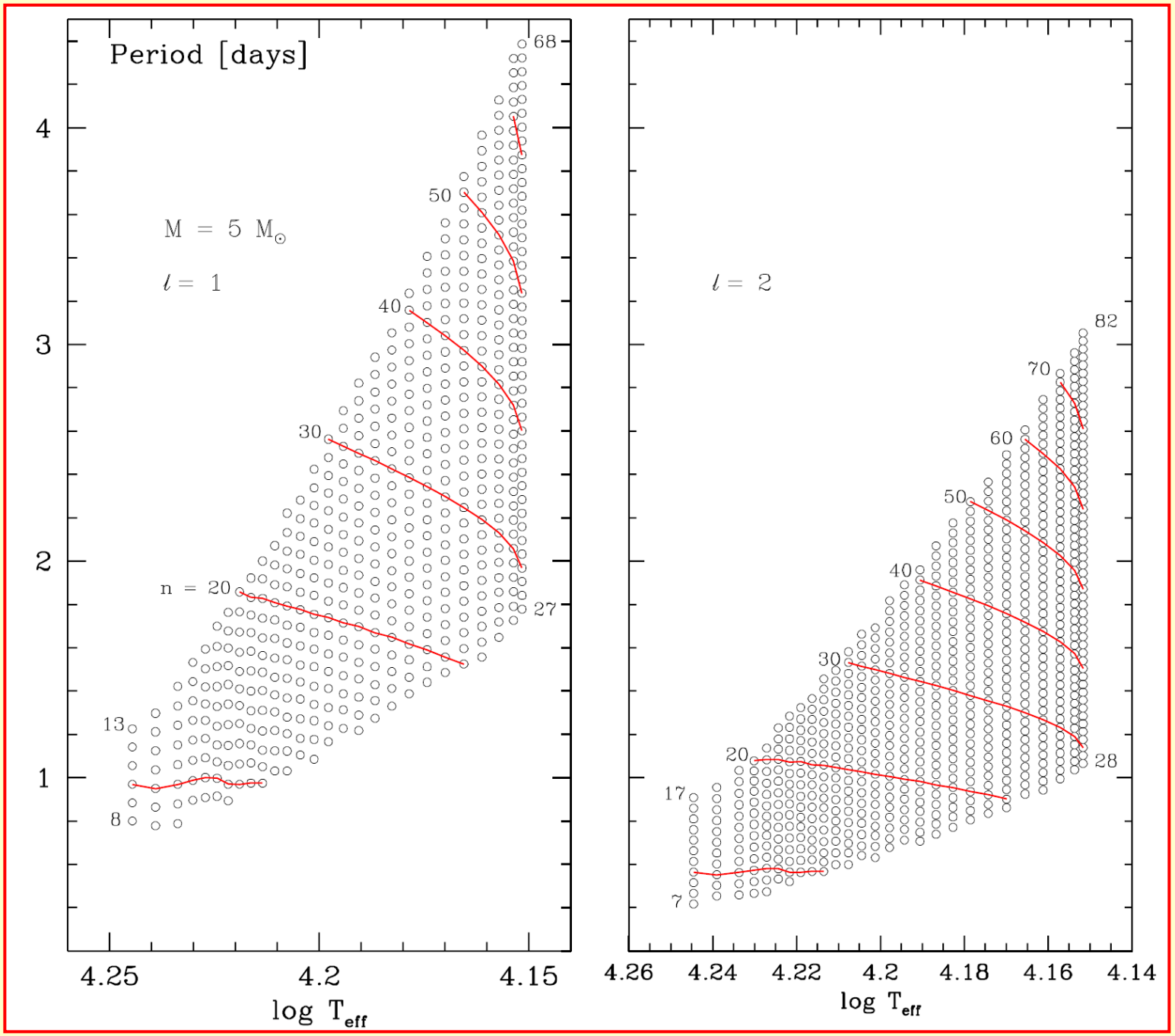

Differential work integral and density of kinetic energy for two modes in the 5 Msun model 70

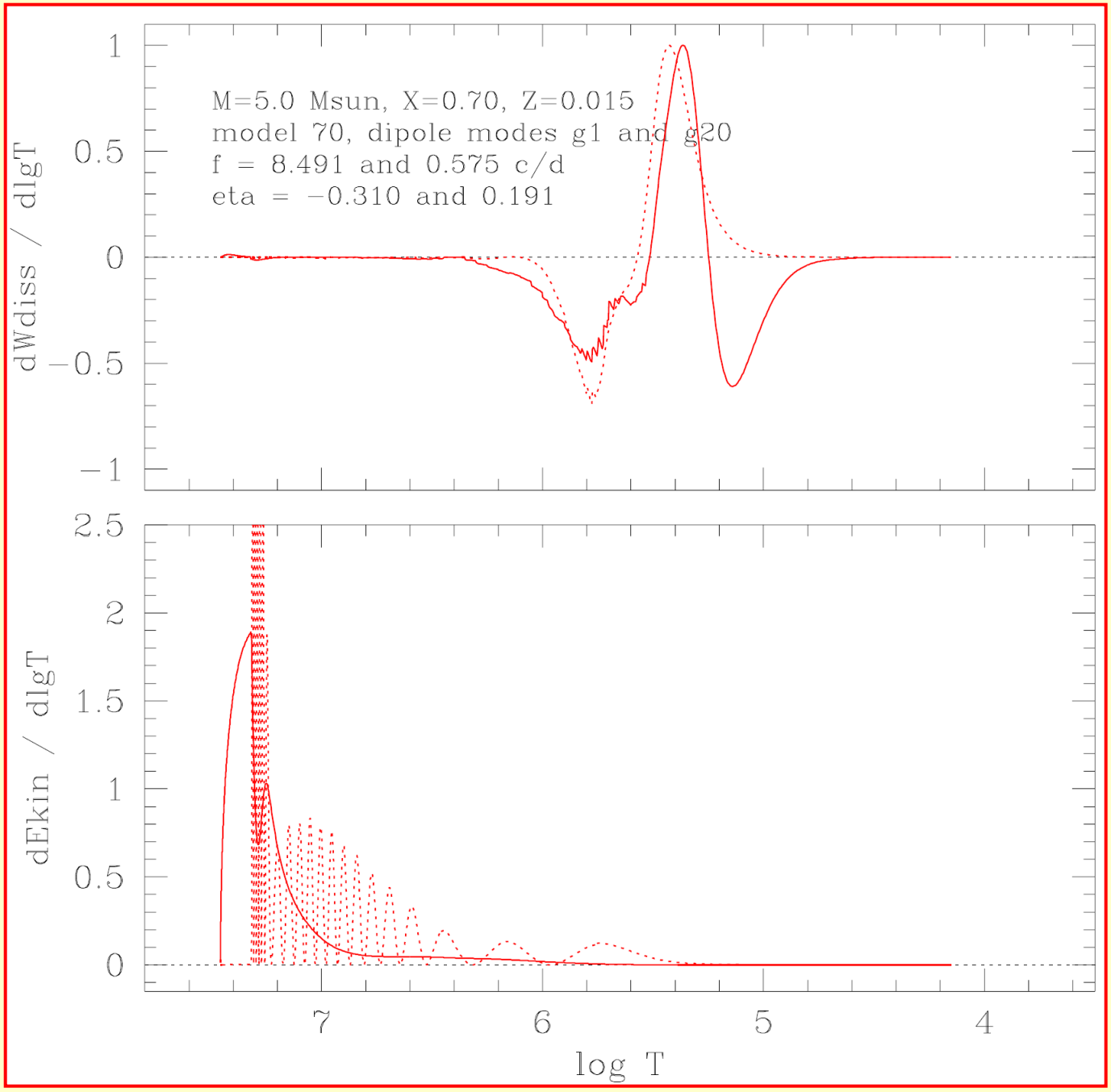

Differential work integral and pressure perturbation for two modes in the 5 Msun model 70

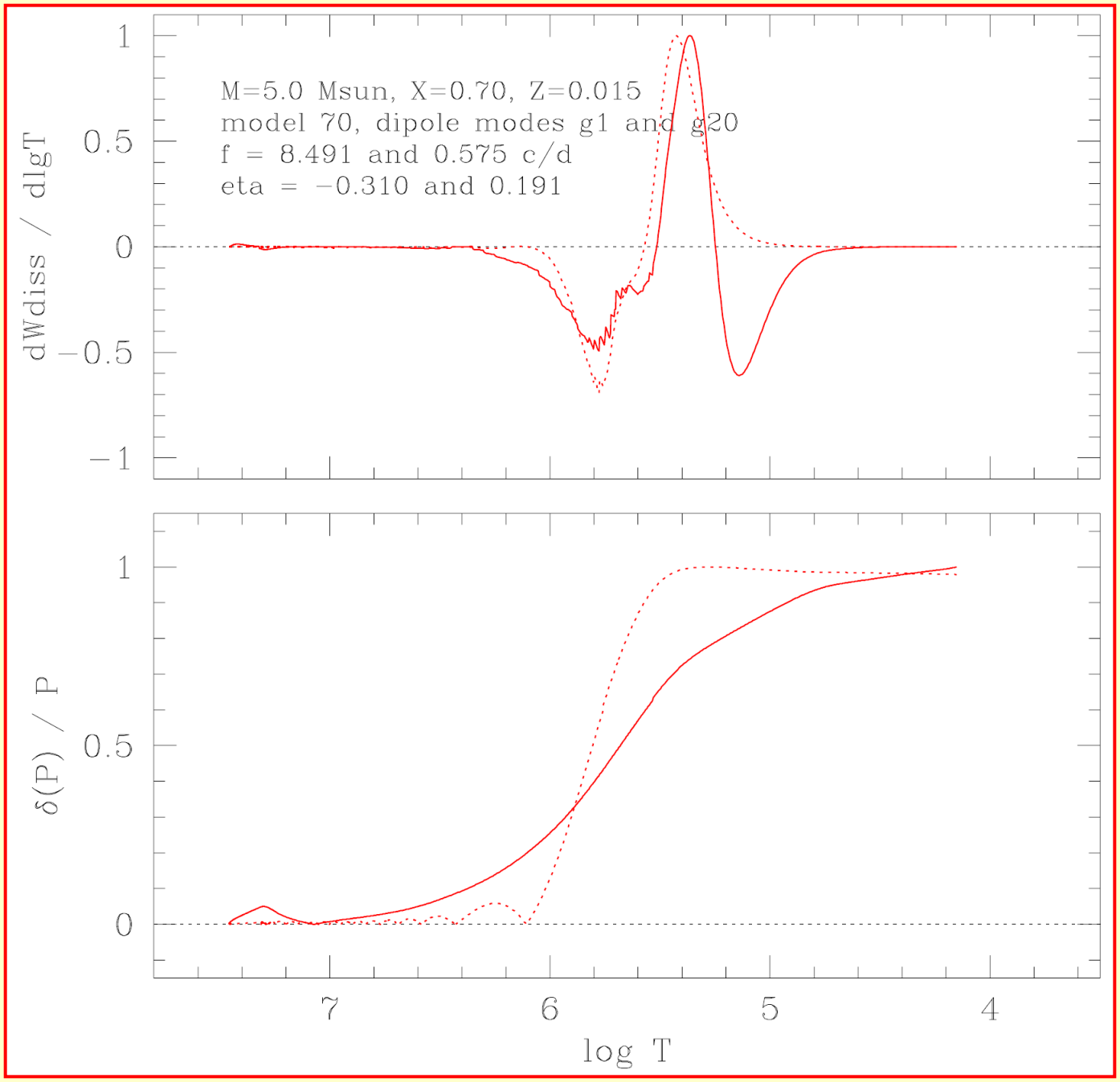

Wybrane modele gwiazd

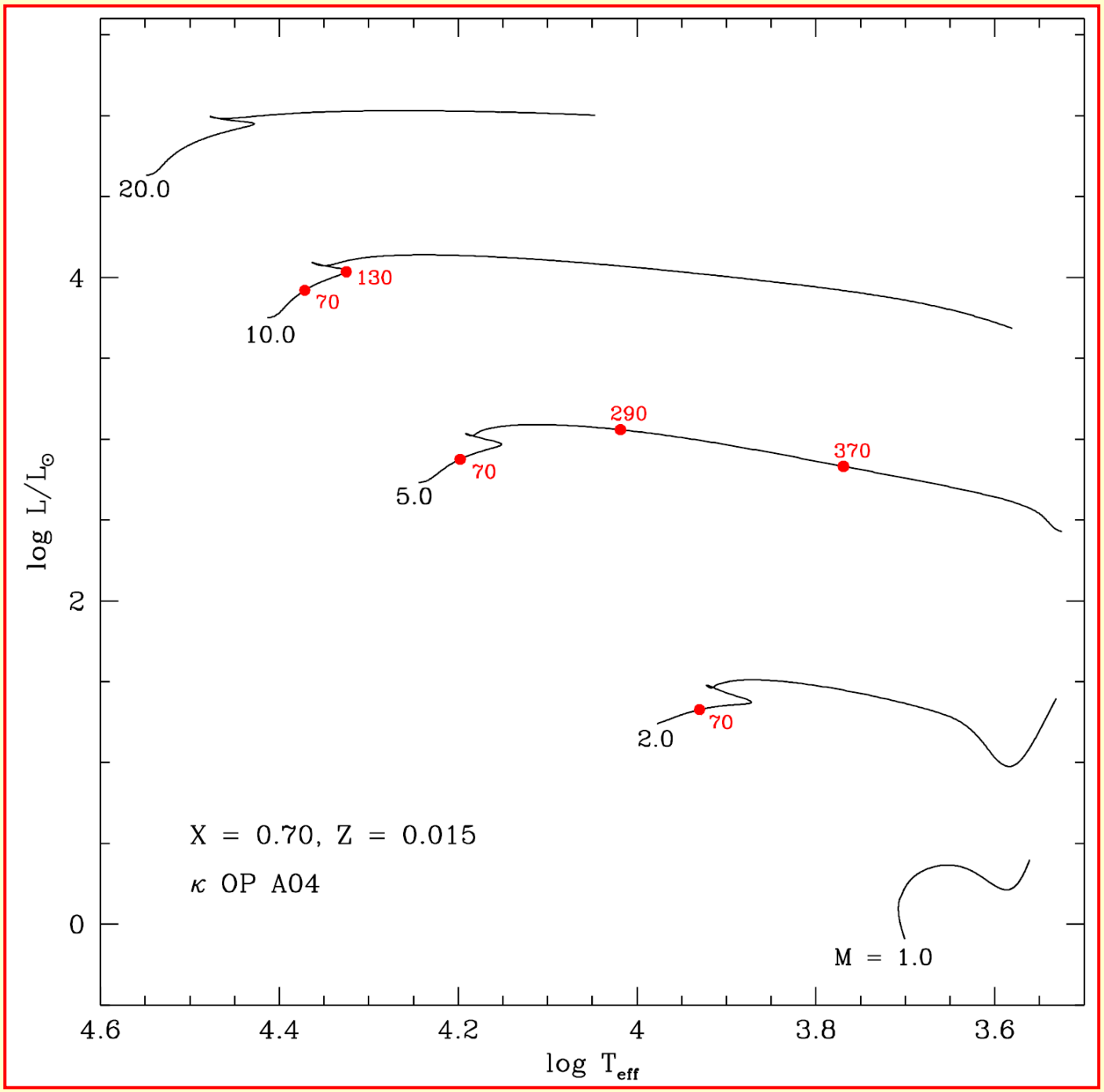

Okresy radialnych, dipolowych i kwadrupolowych oscylacji ewolucyjnych modeli gwiazd z M = 10 Msun (od ZAMS do TAMS)

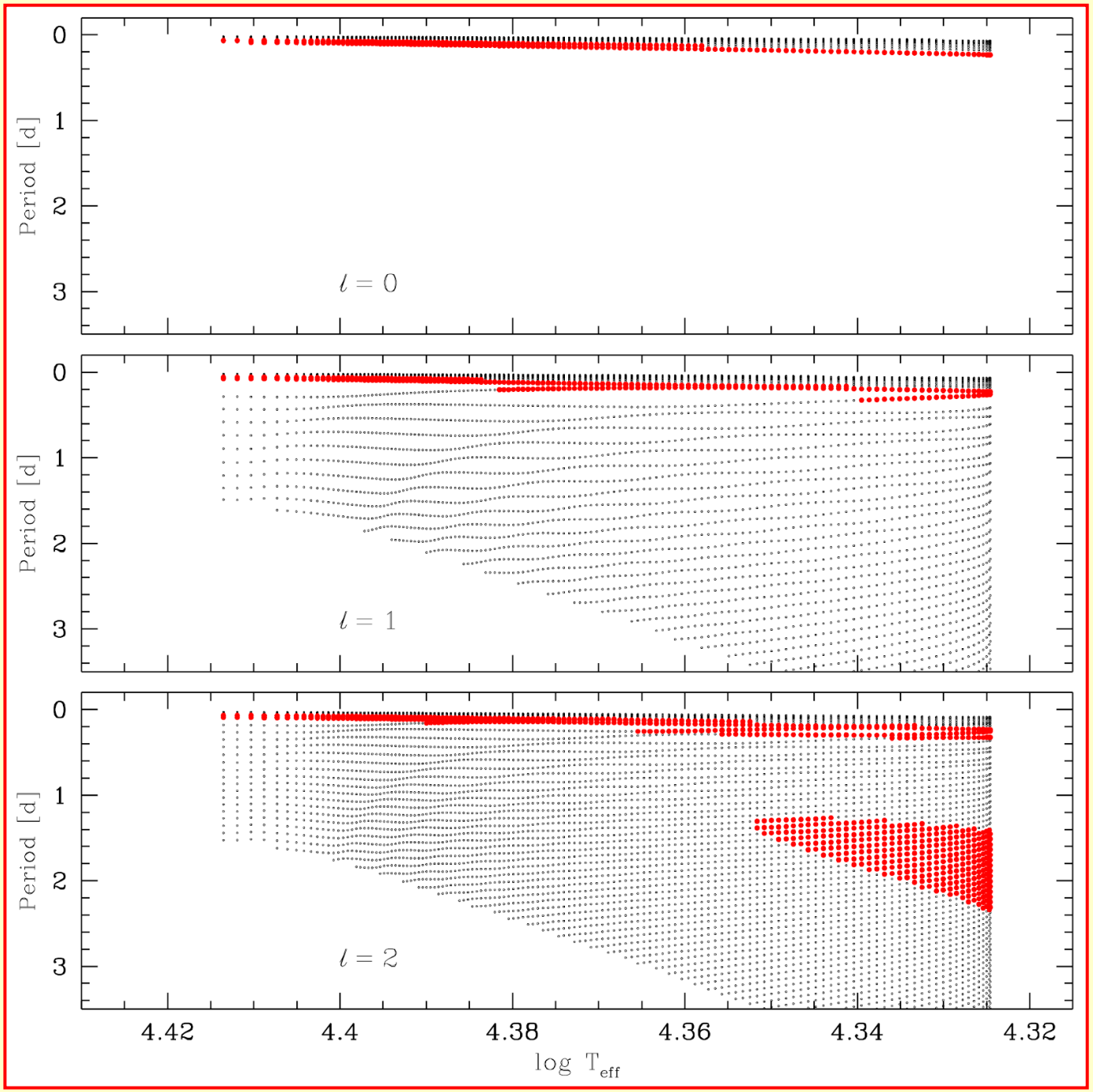

Differential work integral and density of kinetic energy for two modes in the 10 Msun model 130

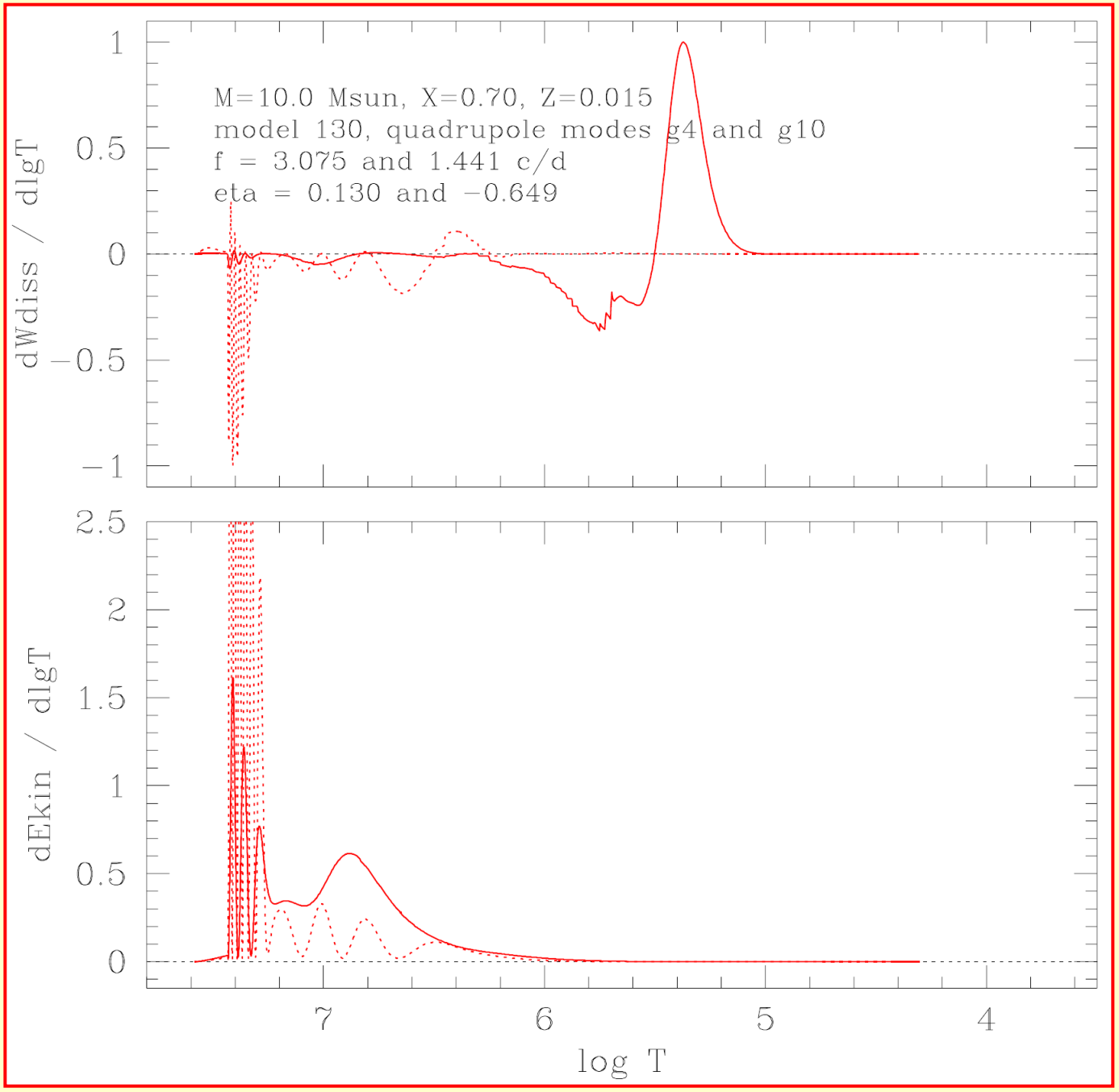

Differential work integral and pressure perturbation for two modes in the 10 Msun model 130

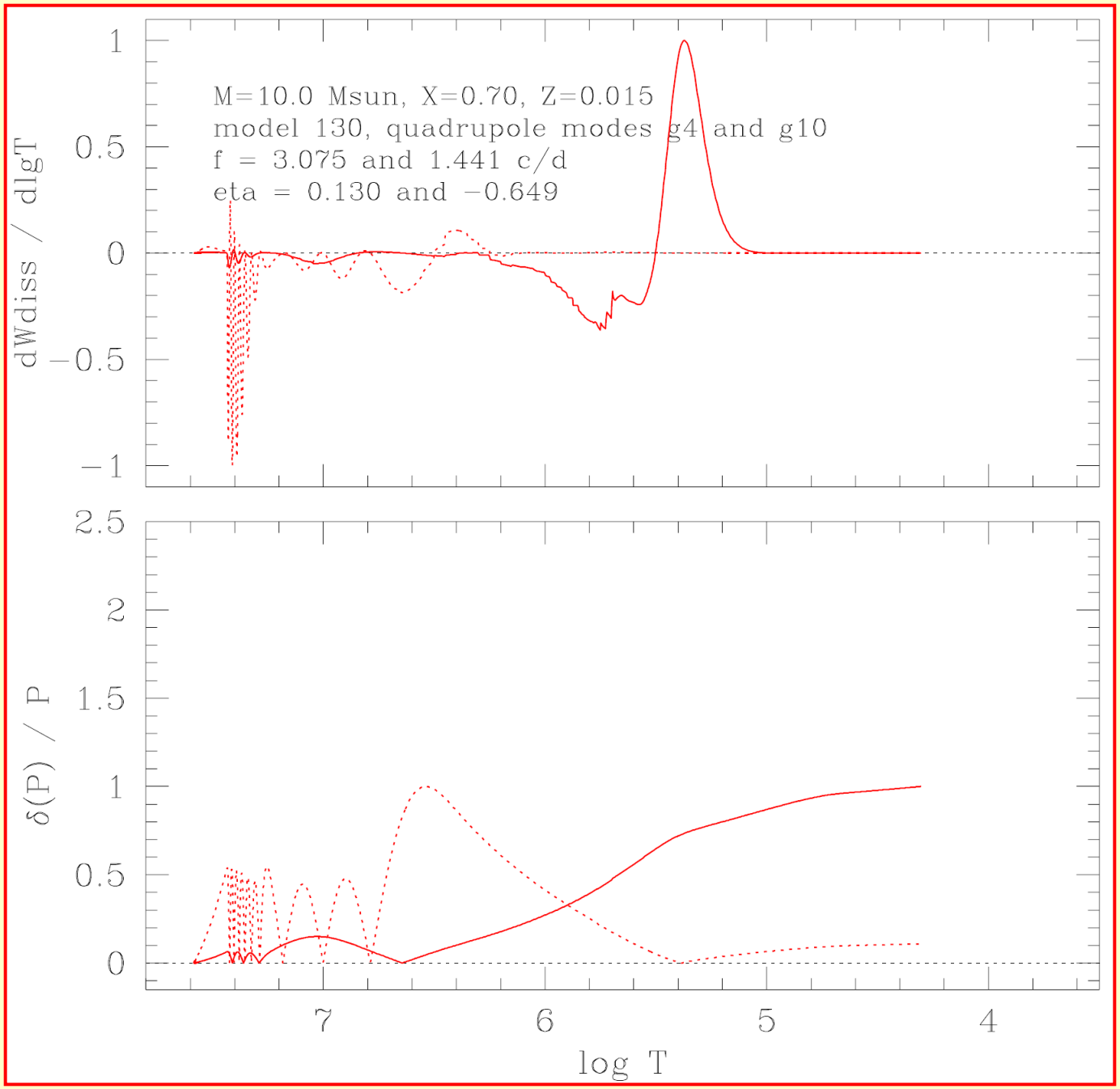

Differential work integral and density of kinetic energy for two modes in the 10 Msun model 130

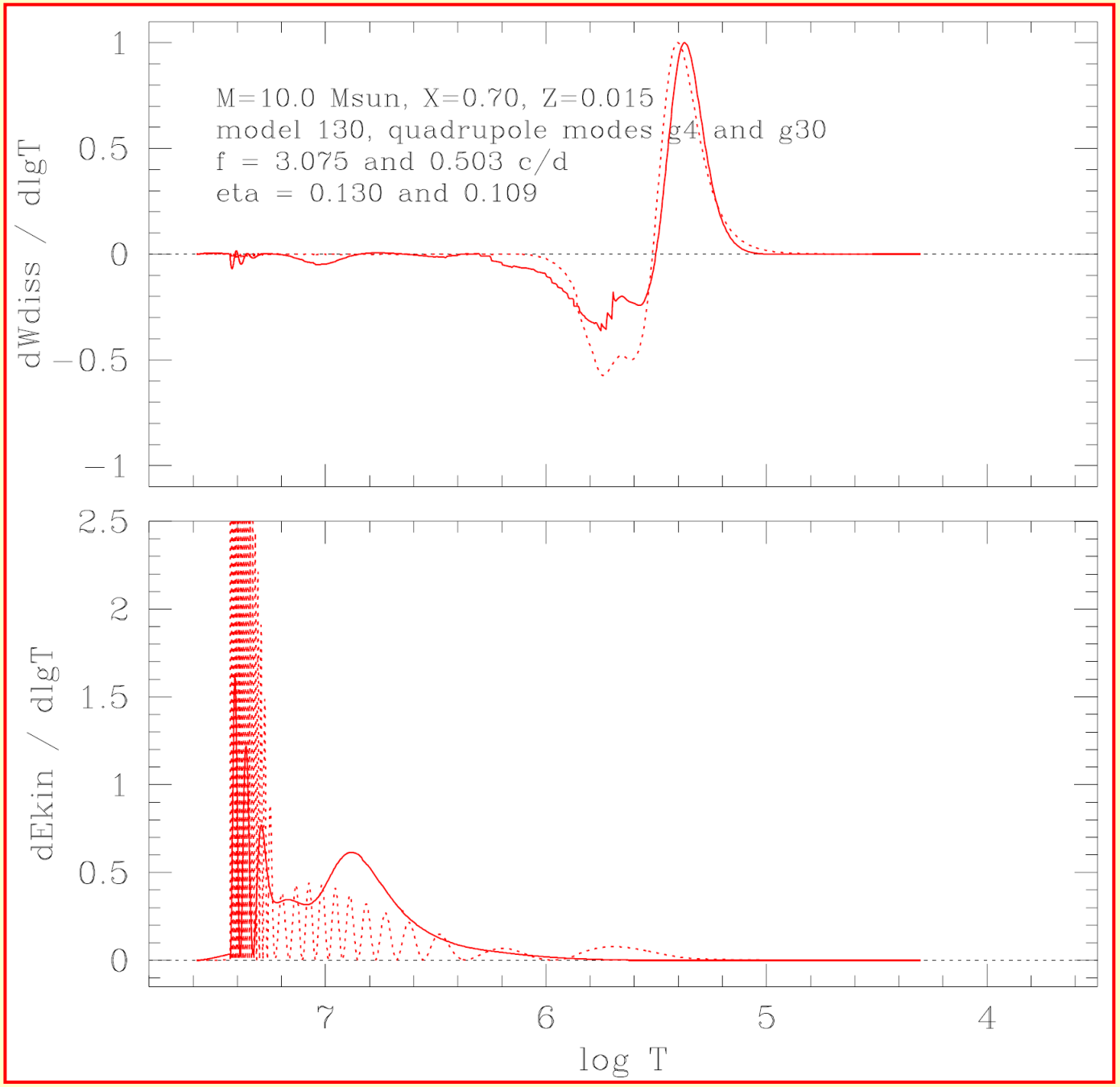

Differential work integral and pressure perturbation for two modes in the 10 Msun model 130

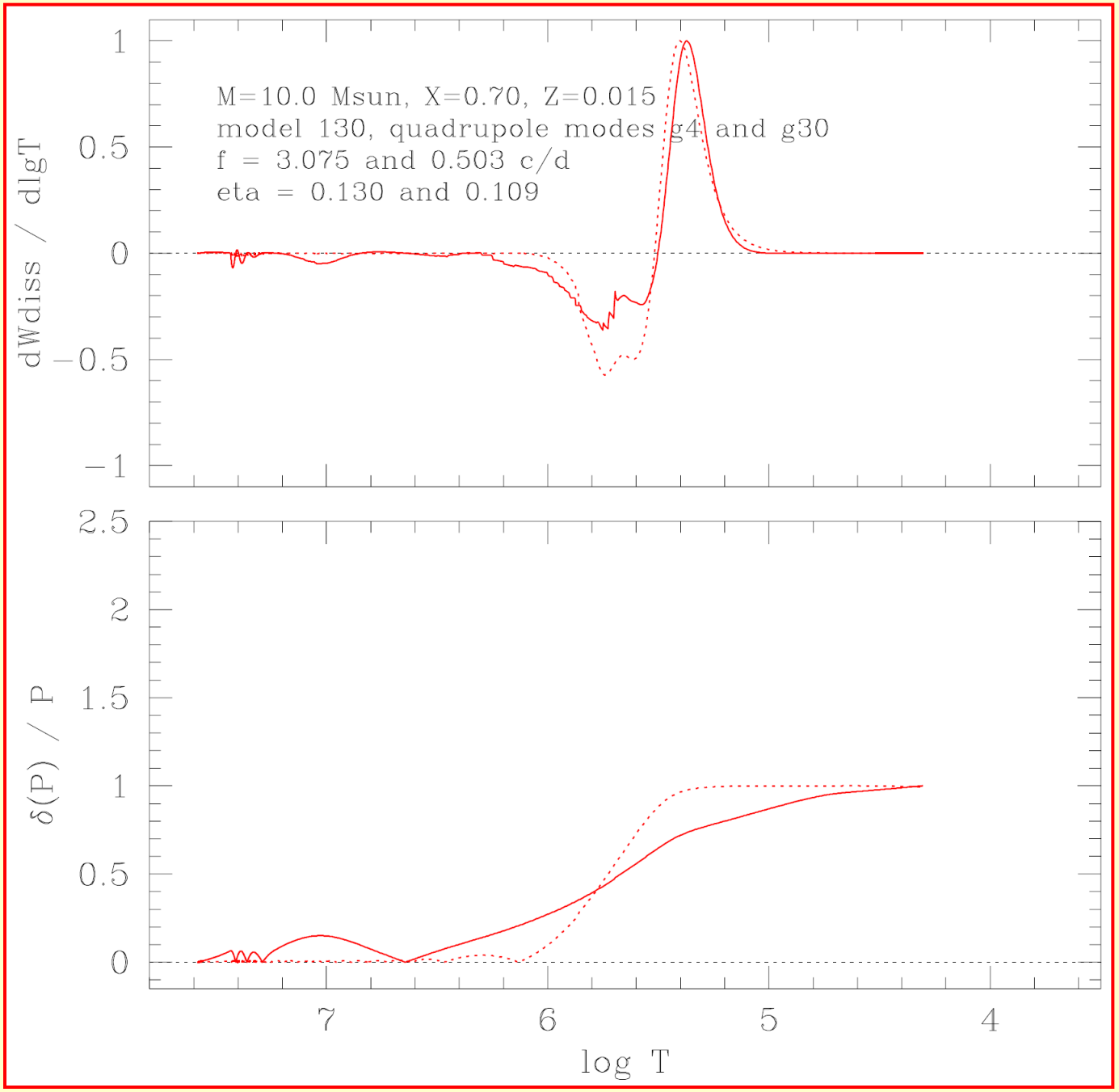

Two frequency ranges of unstable modes (*p* and *g)* in a 30 Msun model

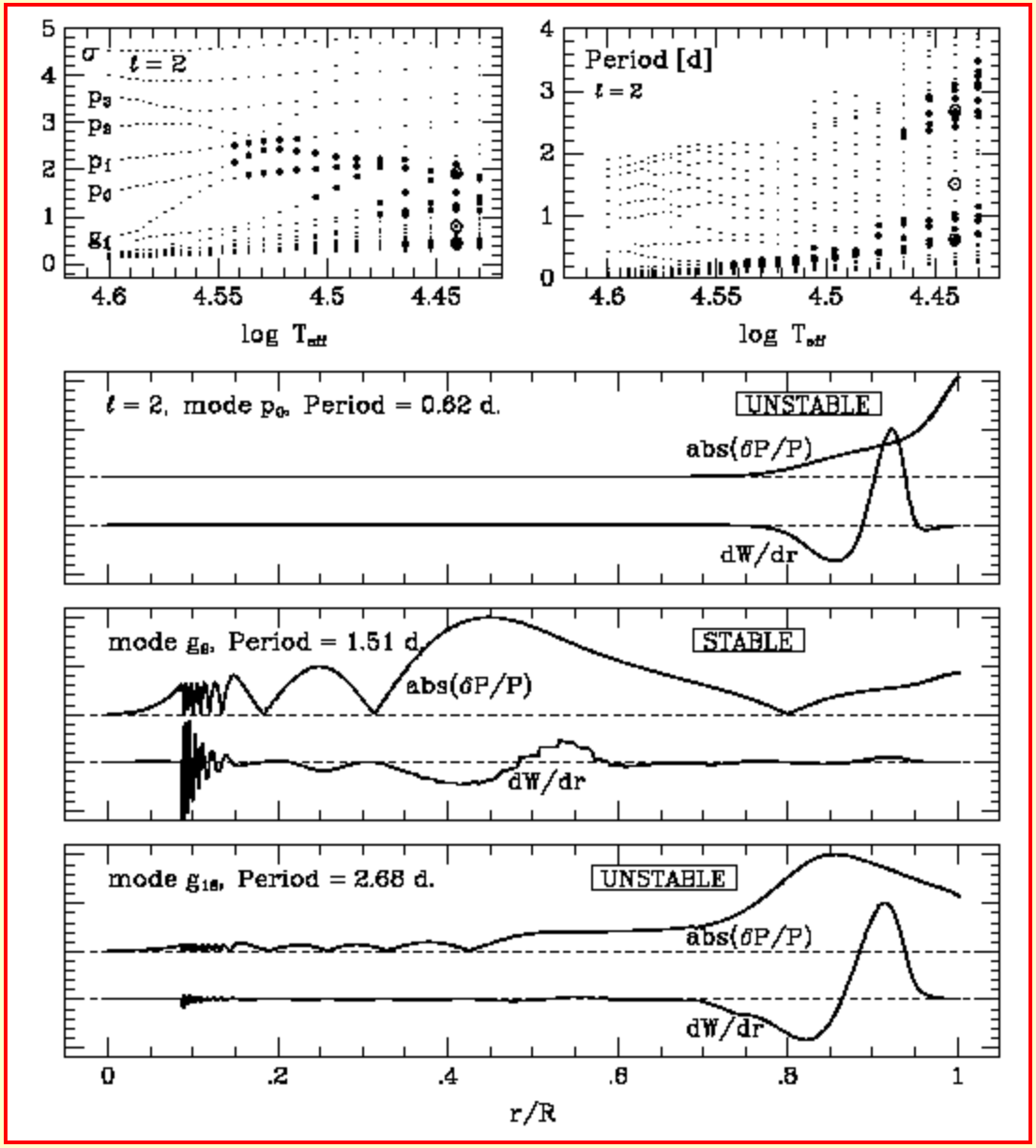

UNSTABLE

STABLE

UNSTABLE

UNSTABLE

STABLE

UNSTABLE

Pamyatnykh, 1999, Acta Astr., 49, 119

Próba wyboru między tablicami OPAL and OP

Hybrydowe oscylacje potencjalnie dają taką możliwość !

$$\eta = \frac{W}{\int_0^1 \left| \frac{dW}{dr} \right| dr}$$

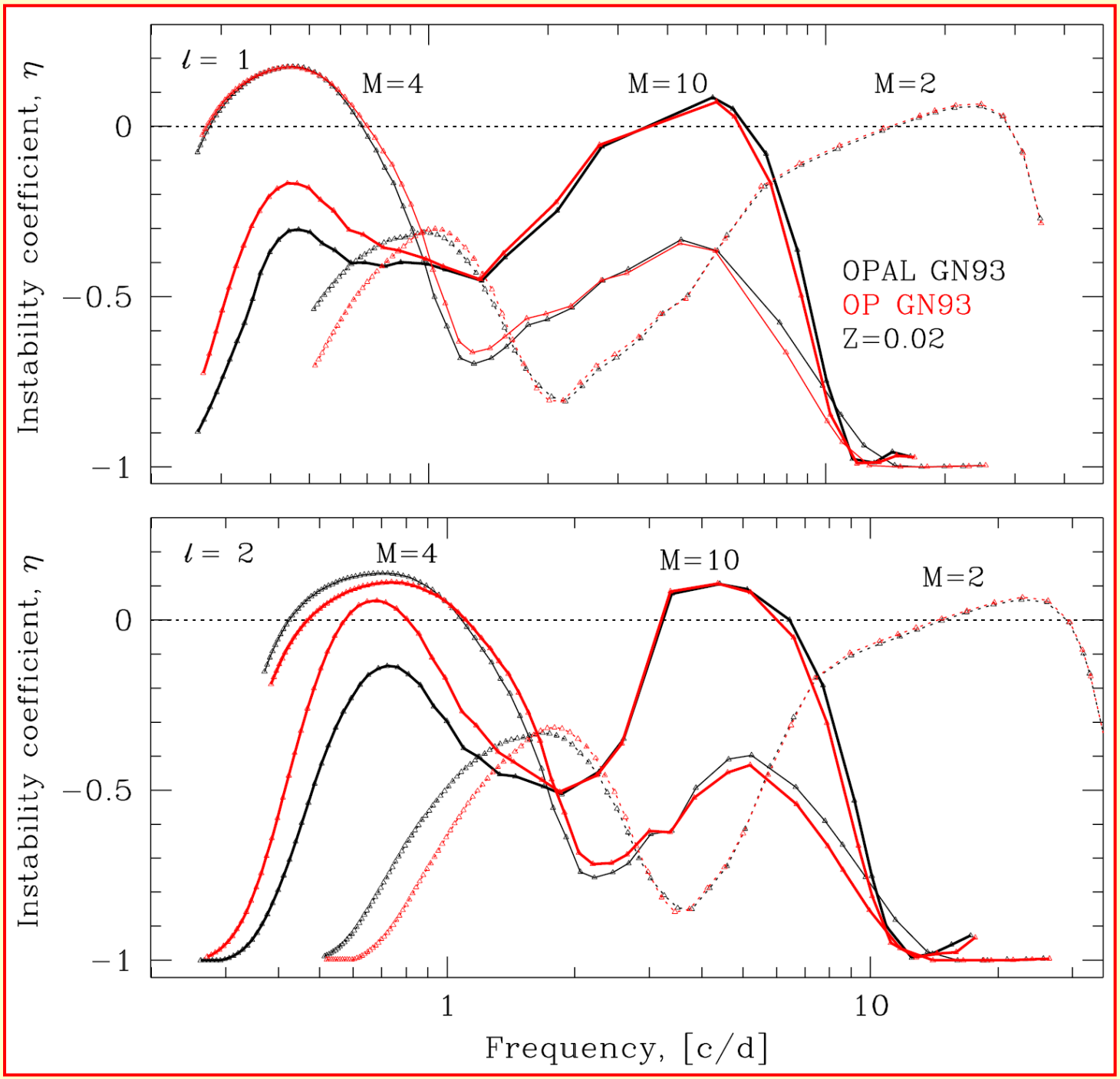

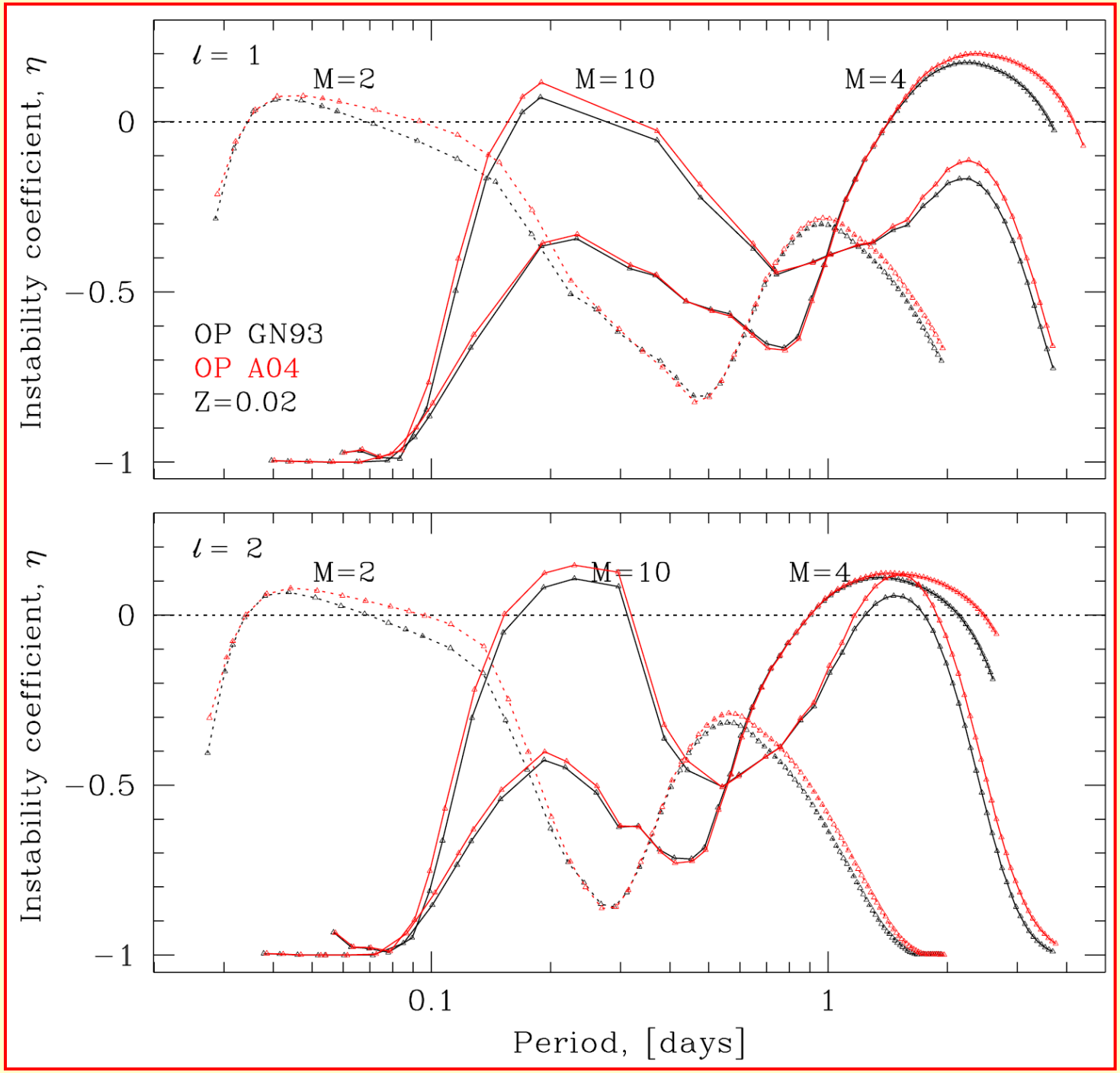
ℓ = 1
M=2
M=10
M=4
OP GN93
OP A04
Z=0.02
Instability coefficient, η
0
−0.5
−1
ℓ = 2
M=2
M=10
M=4
Instability coefficient, η
0
−0.5
−1
0.1
1
Period, [days]

$$\eta = \frac{W}{\int_0^1 \left| \frac{\mathrm{d}W}{\mathrm{d}r} \right| \mathrm{d}r}$$

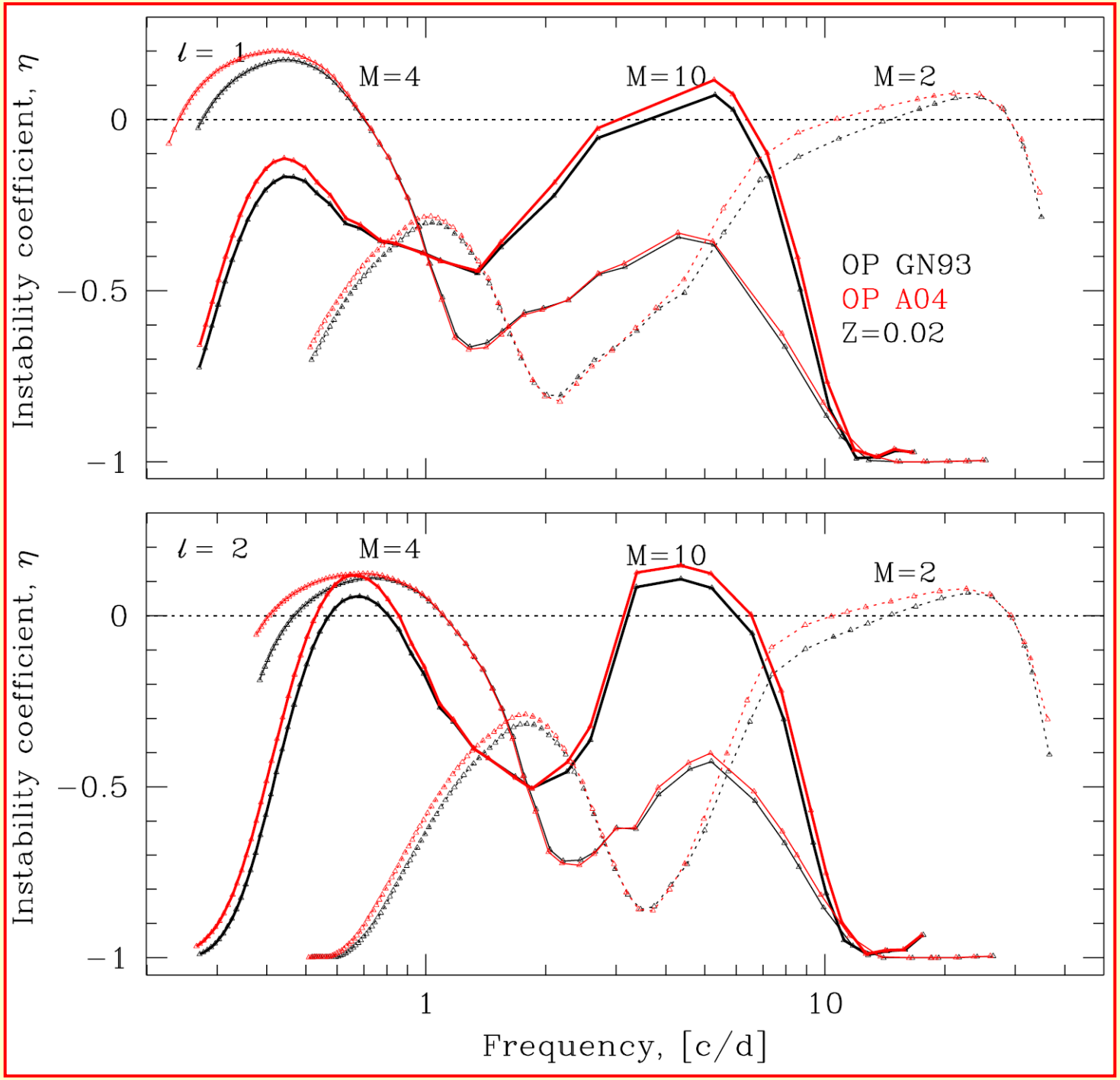

Dwie animacje (autor – Patrick Lenz), przedstawiające MS-ewolucje częstotliwości oraz położenia węzłów p- i g-modów kwadrupulpwych oscylacji wewnątrz modeli gwiazd typu δ Sct i β Cep:

fajle dSct_l2_Lenz.avi i bCep_l2_Lenz.avi (są umieszczone w moim wykładzie na stronie wykładów dla doktorantów)

Fajla dla δ Sct umieszczona również na Youtube:

http://www.youtube.com/watch?v=KOSEtuhXoss

patrick lenz

The END

INSTABILITY DOMAINS IN THE MAIN SEQUENCE

κ OPAL GN93 (Livermore, 1996)

X=0.70, Z=0.02

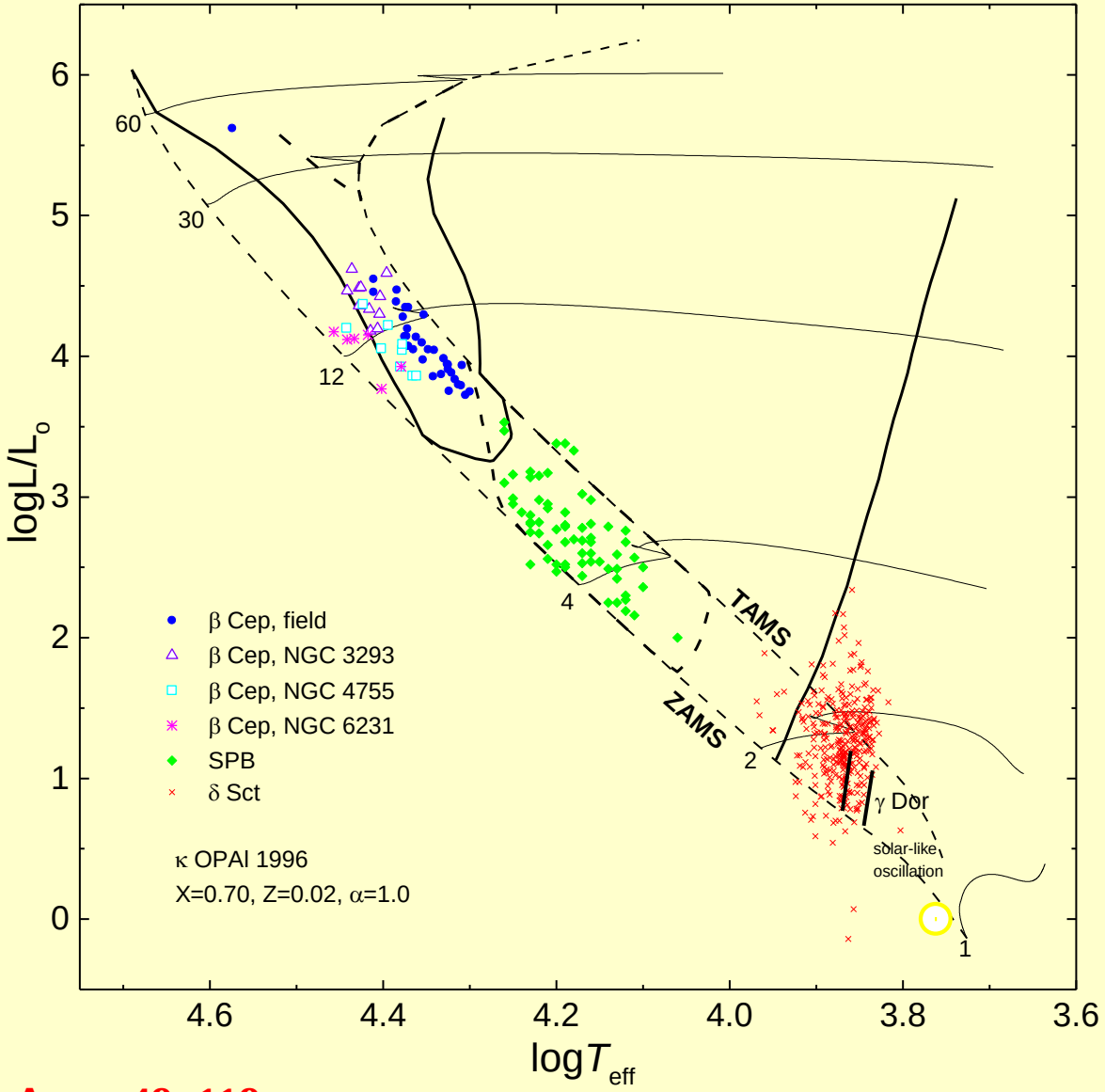

due to Pamyatnykh, 1999, Acta Astr., 49, 119

$$Y_l^m(\theta,\phi) = (-1)^m c_{lm}\ P_l^m\ (\cos\theta)\exp(i\,m\,\phi)$$

$$c_{lm}^2 = \frac{(2l+1)(l-m)!}{4\pi(l+m)!}$$

$$k_{\rm h} = \frac{L}{R}$$

$$\lambda = \frac{2\pi}{k_{\rm h}} = \frac{2\pi R}{L}$$

$$t_{\rm dyn} \simeq \left(\frac{R^3}{GM}\right)^{1/2} \simeq (G\bar{\rho})^{-1/2}$$

$$Q = \Pi \left(\frac{M}{M_\odot}\right)^{1/2} \left(\frac{R}{R_\odot}\right)^{-3/2}$$

- Effective gravity:

$$g_{eff} = g - \frac{2}{3}\Omega^2 r$$

- Ledoux constant:

$$C_{nl} = \frac{\int (2yz + z^2)\rho r^4 dr}{\int (y^2 + \Lambda z^2)\rho r^4 dr} \qquad \Lambda = l(l+1)$$

y, z – radial and horizontal components of displacement

$C_{nl} \ll 1$ for high-order p-modes $(y \gg z)$

$C_{nl} \simeq \frac{1}{l(l+1)}$ for g-modes $(z \gg y)$

$C \sim \frac{1}{2}$ for gravity modes of $l = 1$

Stars whose luminosity varies periodically have been known for centuries. However, only within the last hundred years has it been definitely established that in many cases these variations are due to *intrinsic* pulsations of the stars themselves. For obvious reasons studies of pulsating stars initially concentrated on stars with large amplitudes, such as the Cepheids and the long period variables. The variations of these stars could be understood in terms of pulsations in the fundamental radial mode, where the star expands and contracts, while preserving spherical symmetry. It was realized very early (Shapley 1914) that the period of such motion is approximately given by the dynamical time scale of the star:

$$t_{\rm dyn} \simeq \left(\frac{R^3}{GM}\right)^{1/2} \simeq (G\bar{\rho})^{-1/2} \,, \tag{1.1}$$

where R is the radius of the star, M is its mass, $\bar{\rho}$ is its mean density, and G is the gravitational constant. Thus observation of the period immediately gives an estimate of one intrinsic property of the star, *viz.* its mean density.

It is a characteristic property of the Cepheids that they lie in a narrow, almost vertical strip in the HR diagram, the so-called *instability strip*. As a result, there is a direct relation between the luminosities of these stars and their radii; assuming also a mass-luminosity relation one obtains a relation between the luminosities and the periods, provided that the latter scale as $t_{\rm dyn}$. This argument motivates the existence of a *period-luminosity relation* for the Cepheids: thus the periods, which are easy to determine observationally, may be used to infer the intrinsic luminosities; since the apparent luminosities can be measured, one can determine the distance to the stars. This provides one of the most important distance indicators in astrophysics.

The main emphasis in the early studies was on understanding the causes of the pulsations, particularly the concentration of pulsating stars in the instability strip. As in many other branches of astrophysics major contributions to the understanding of stellar pulsation were made by Eddington (*e.g.* Eddington 1926). However, the identification of the actual cause of the pulsations, and of the reason for the instability strip, was first arrived at independently by Zhevakin (1953) and by Cox & Whitney (1958).

Avoided crossing, testing overshooting

Frequencies of dipole and quadrupole modes for models of a 2 Msun in the MS evolutionary stage (from ZAMS to TAMS)

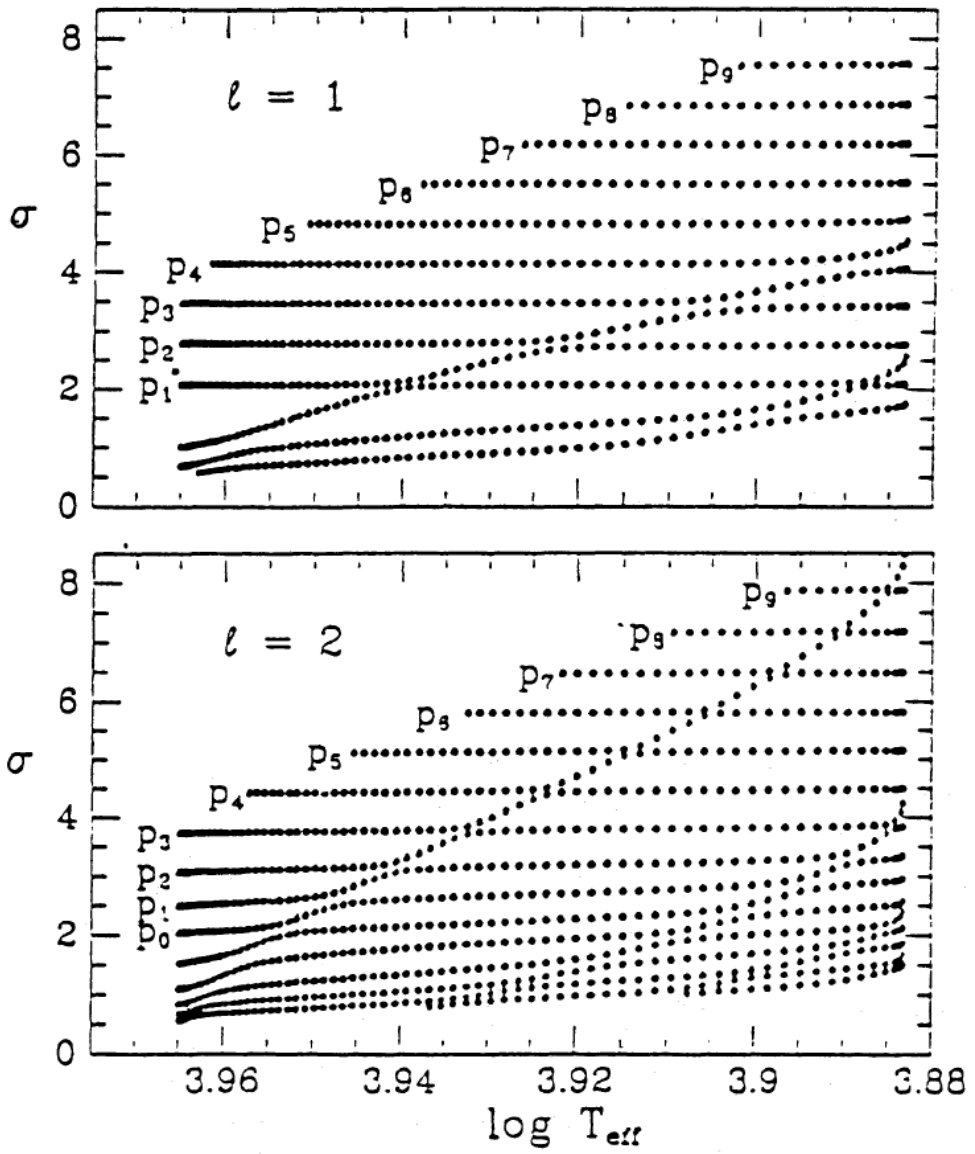

Fig.1 Dimensionless frequences of low order modes corresponding to $l = 1$ and 2 spherical harmonics for models of a $2M_{\odot}$ star in the Main-Sequence evolutionary phase. Pulsation instability begins at $\log T_{\rm eff} \approx 3.94$.

Dziembowski & Pamyatnykh 1991

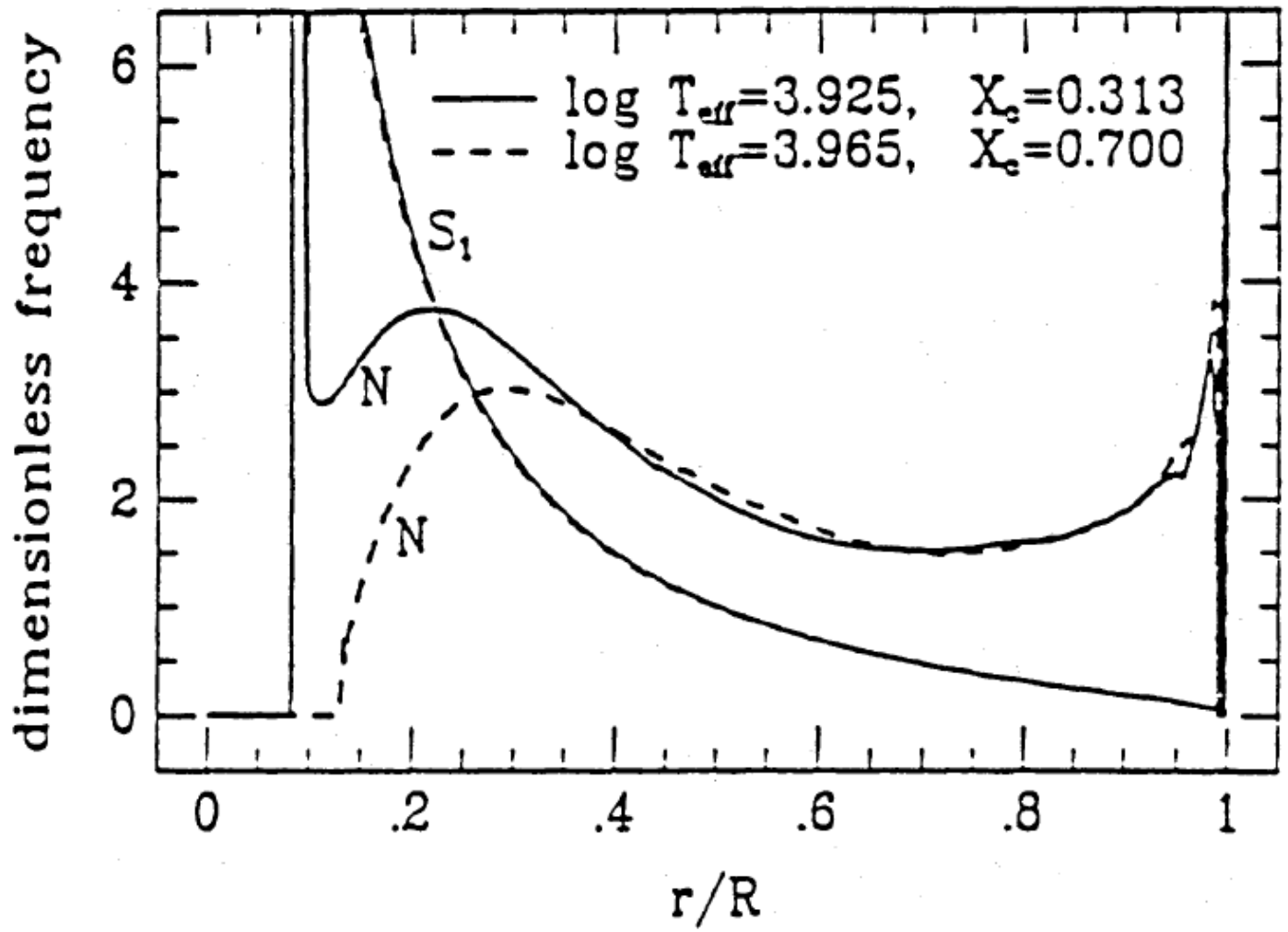

Fig.2 Brunt-Väisälä and Lamb frequencies in two models of $2M_\odot$ during the Main Sequence evolution. The frequencies are expressed in the $\sqrt{4\pi G<\rho>}$ units. Maximum value of N in the interior of the evolved model is ≈ 12.

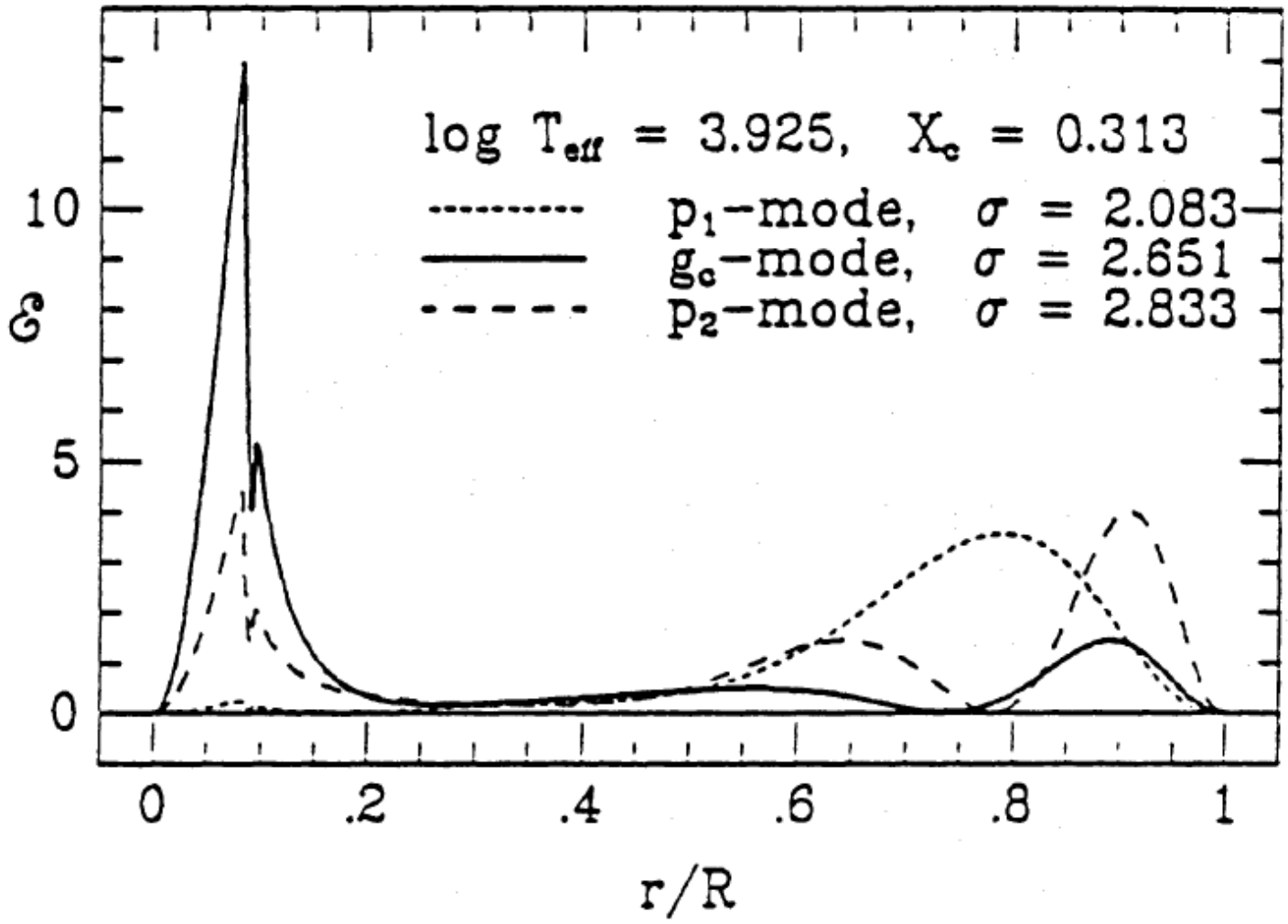

Fig.3 Kinetic energy density for for g_c- mode and two neighbouring p-modes. Normalization $\int_0^1 \mathcal{E} dx = 1$ is adopted. The inner maximum of $\mathcal{E}$ occurs at the boundary of the convective core.

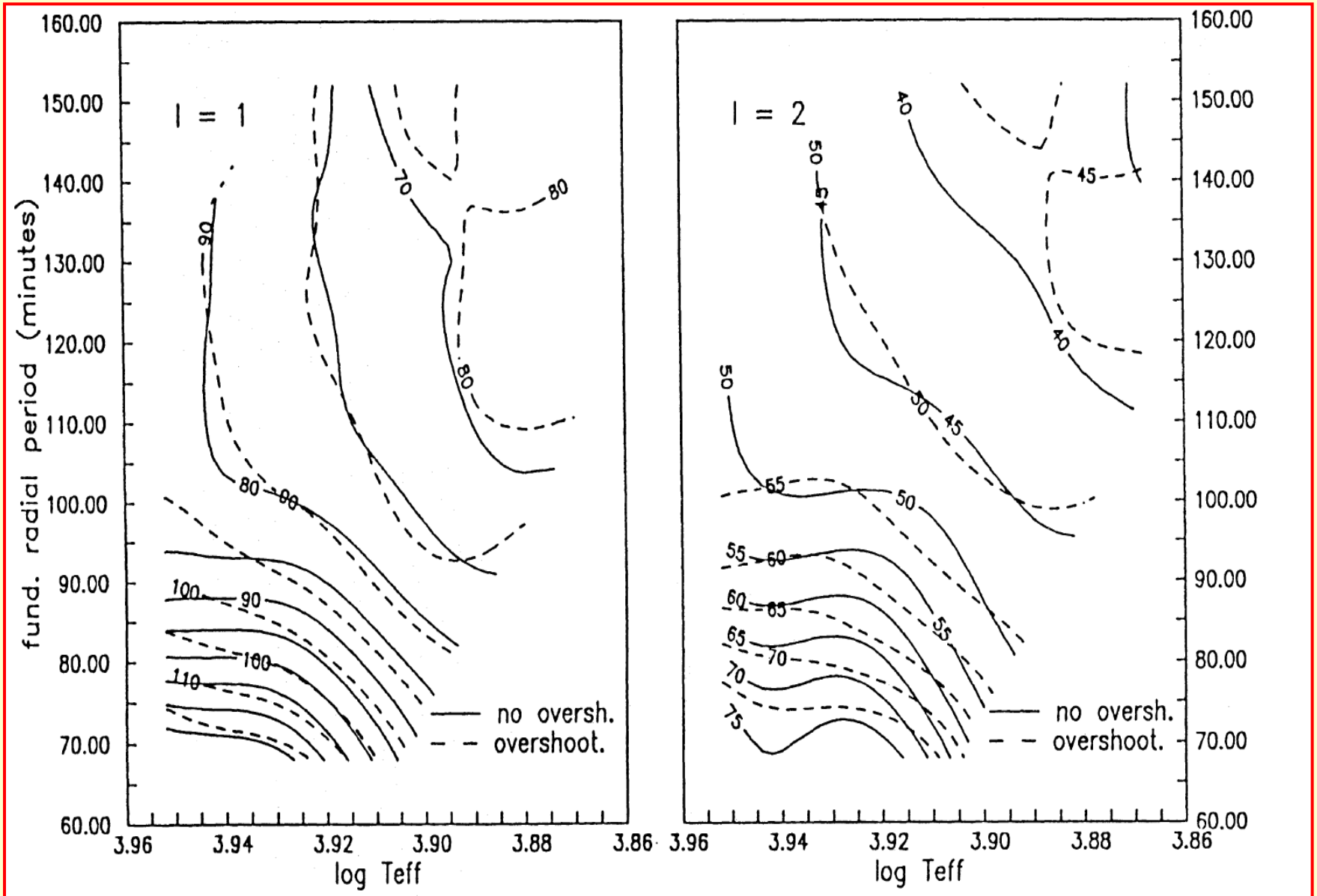

Fig.4 Lines of constant of g_c-mode period (in minutes) obtained for sequences of Main Sequence stellar models with $M = 1.8{-}2.2M_\odot$ calculated by assuming no overshooting (continues lines) and overshooting with a distance $d_{\rm over} \approx 0.25H_p$ (dashed lines).